

UCL

Université
catholique
de Louvain

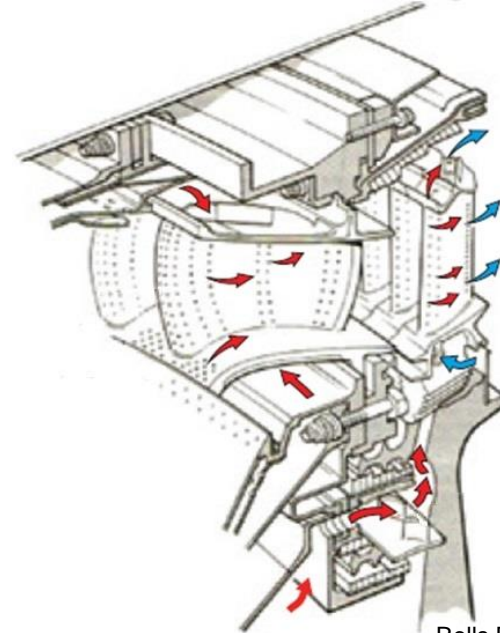
fnrs
LA LIBERTÉ DE CHERCHER



LIF Temperature field Measurements for Internal Forced Convection Blade Cooling

Gian Luca Gori

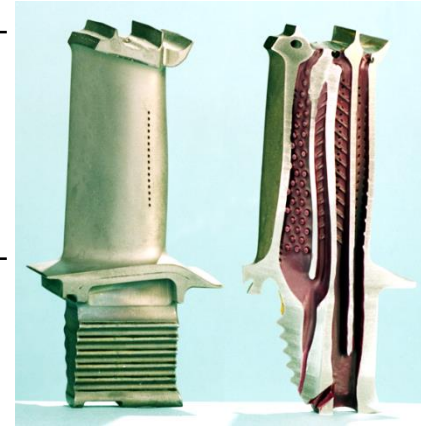
Supervisor: Tony Arts



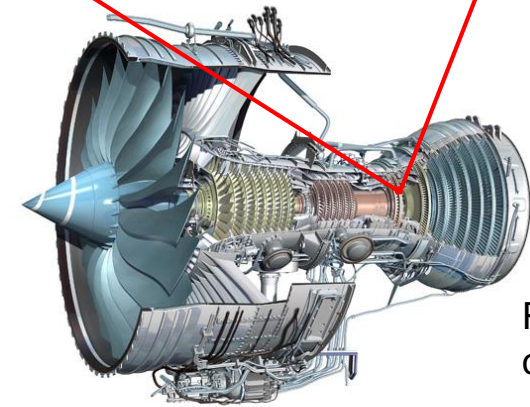
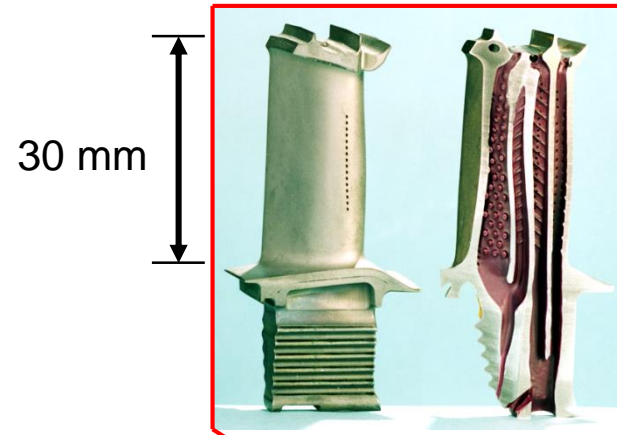
Rolls Royce - The Jet Engine

Contest: Cooling in HP Turbine Blades

30 mm



Contest: Cooling in HP Turbine Blades

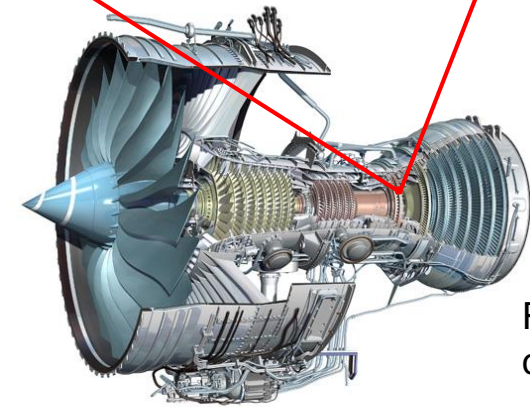
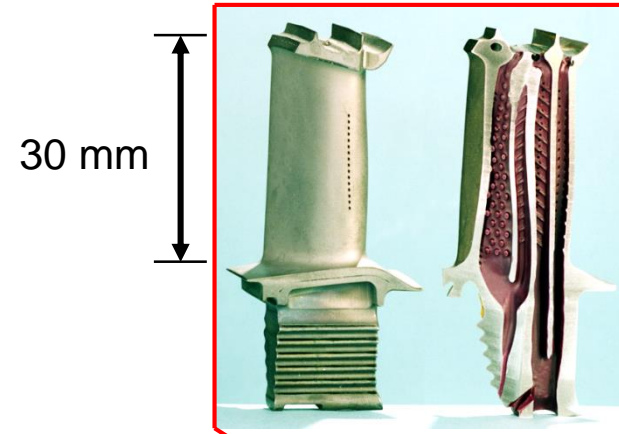


RR Trent 1000
cutaway



Contest: Cooling in HP Turbine Blades

- ❑ High load (almost $\frac{1}{2}$ of enthalphy drop in 1 or maximum 2 stages)

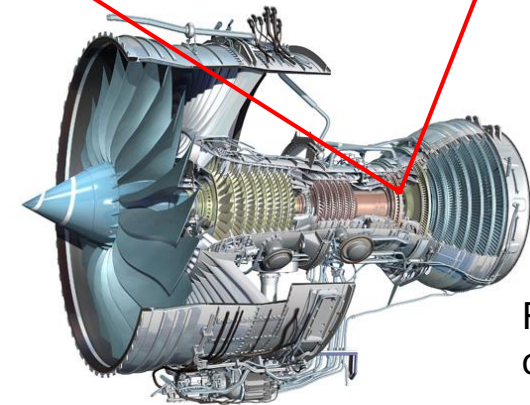
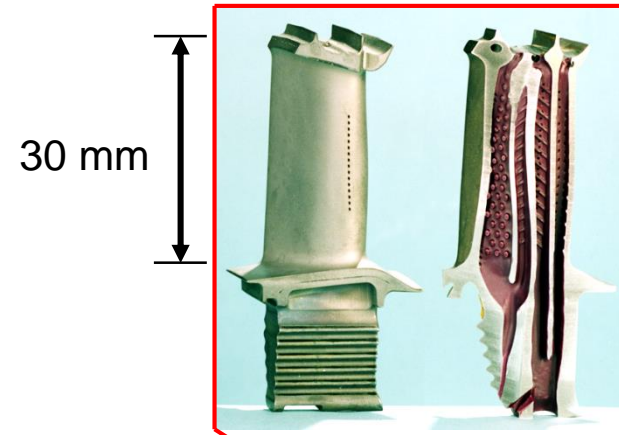


RR Trent 1000
cutaway



Contest: Cooling in HP Turbine Blades

- ❑ High load (almost $\frac{1}{2}$ of enthalphy drop in 1 or maximum 2 stages)
- ❑ Higher **TIT** (~ 1600 °C) allows better performance
- vs
- ❑ **thermal resistance** (< 1000 °C) + **mechanical stresses**
 - **Materials & Cooling**
- ❑ Longer Life-time ($\sim 10^4$ hours)
 - lower replacement costs (~ 10 k€ / airfoil)



RR Trent 1000 cutaway



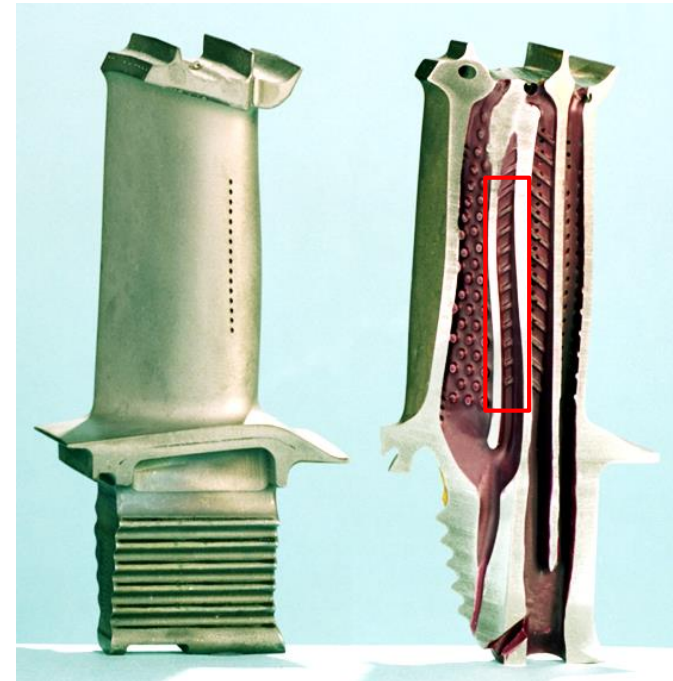
Internal Cooling by Forced Convection

- ❑ Wide literature
- ❑ Complex 3D and unsteady flow
- ❑ Heat transfer prediction accuracy by RANS

≈ 10÷15%

(most of the time based on isotropic turbulence and constant Pr_t)

- ❑ Demands
 - Understanding of the physics
 - Experimental data support for CFD improvements



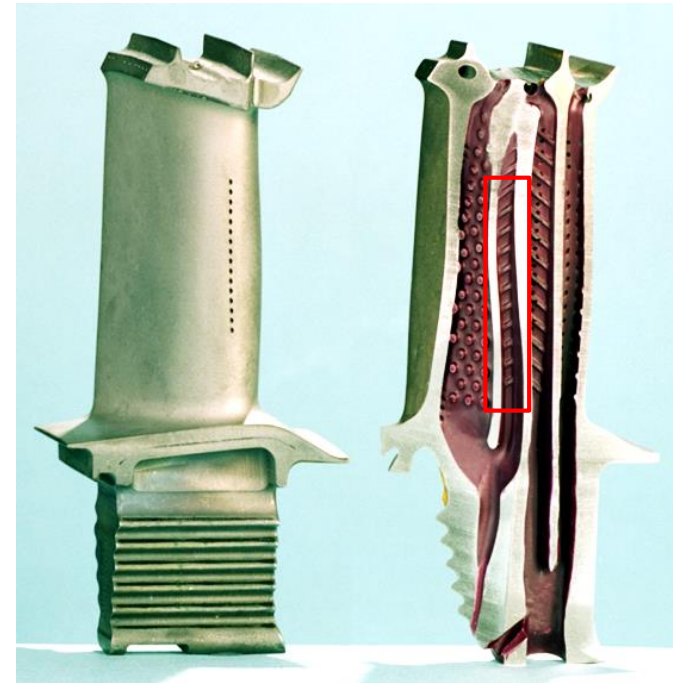
Internal Cooling by Forced Convection

- ❑ Wide literature
- ❑ Complex 3D and unsteady flow
- ❑ Heat transfer prediction accuracy by RANS

≈ 10÷15%

(most of the time based on isotropic turbulence and constant Pr_t)

- ❑ Demands
 - Understanding of the physics
 - Experimental data support for CFD improvements

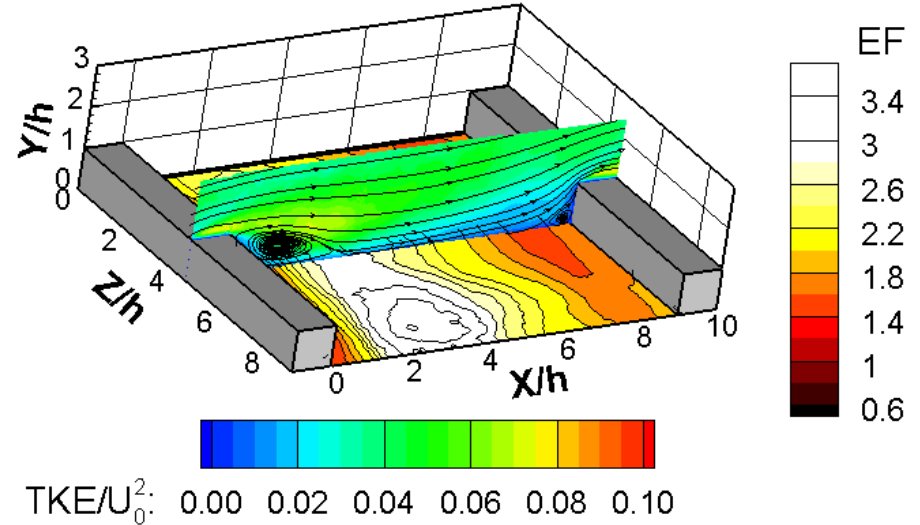


Research Contribution

High accuracy, high resolution and detailed measurements

Goals

- ❑ Intermediate link between Heat Transfer and Flow velocity measurements (available in literature) by **Flow Temperature Data**
- ❑ Contribution on **Reynolds stresses** and **turbulent heat transport term**
- ❑ Determination of the turbulent eddy viscosity and turbulent thermal diffusivity \Rightarrow **turbulent Prandtl number**



Momentum and thermal equation

$$\bar{u} \frac{\partial \bar{u}}{\partial x} + \bar{v} \frac{\partial \bar{u}}{\partial y} = -\frac{1}{\rho} \frac{d\bar{P}}{dx} + \frac{\partial}{\partial y} \left(\nu \frac{\partial \bar{u}}{\partial y} - \overline{u'v'} \right)$$

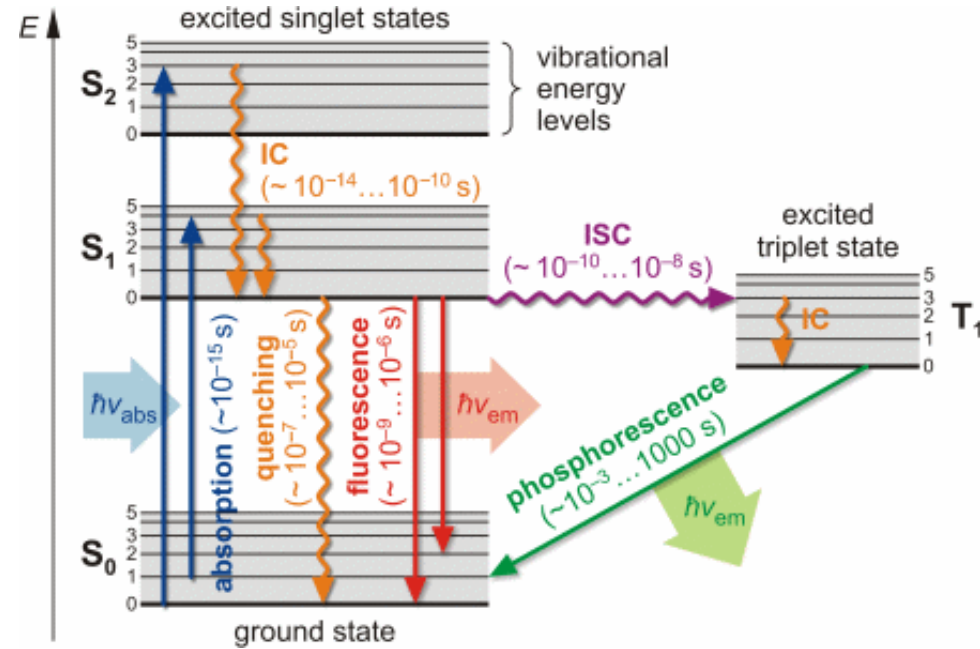
$$\bar{u} \frac{\partial \bar{T}}{\partial x} + \bar{v} \frac{\partial \bar{T}}{\partial y} = \frac{\partial}{\partial y} \left(\alpha \frac{\partial \bar{T}}{\partial y} - \overline{v'T'} \right)$$

$$Pr_t = \frac{\mu_t}{\alpha_t} = \frac{\overline{u'v'}/\frac{\partial \bar{u}}{\partial y}}{\overline{v'T'}/\frac{\partial \bar{T}}{\partial y}}$$

LIF thermography

□ Choice of the technique

- Non-intrusive
- 2D measurements



Signal

$$1\text{-color: } I_f(\lambda) = K_{opt}(\lambda)K_{spec}(\lambda)V_c I_1 C e^{\beta(\lambda)/T}$$

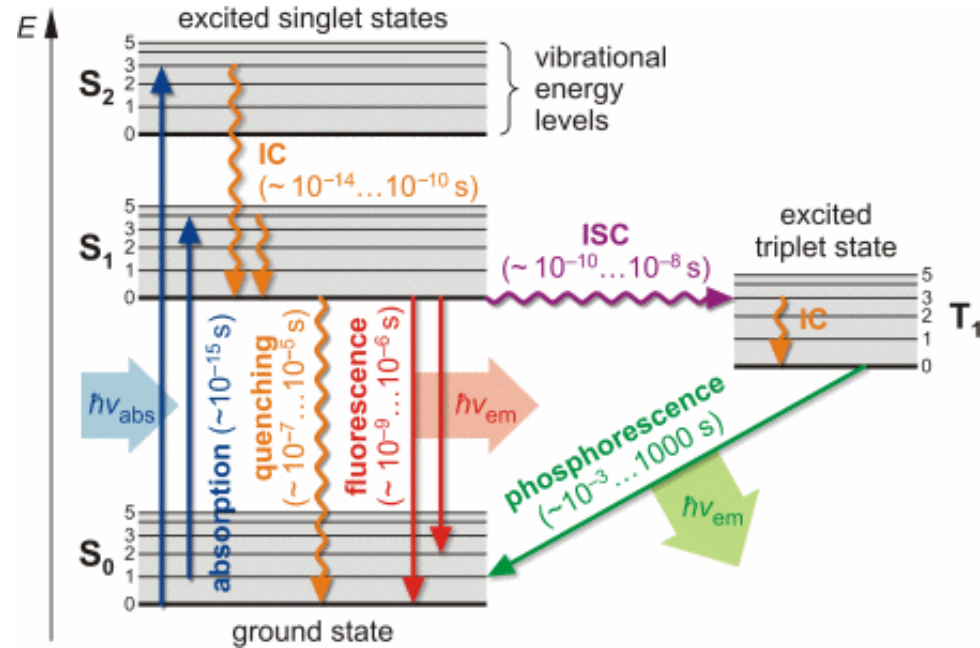
LIF thermography

Choice of the technique

- Non-intrusive
- 2D measurements

Laser intensity & Tracer concentration variations?

- $I_1 = f(t) \rightarrow$ reference to normalize
- C depends on the local mixing



Signal



1-color: $I_f(\lambda) = K_{opt}(\lambda)K_{spec}(\lambda)V_d I_1 C e^{\beta(\lambda)/T}$

LIF thermography

Choice of the technique

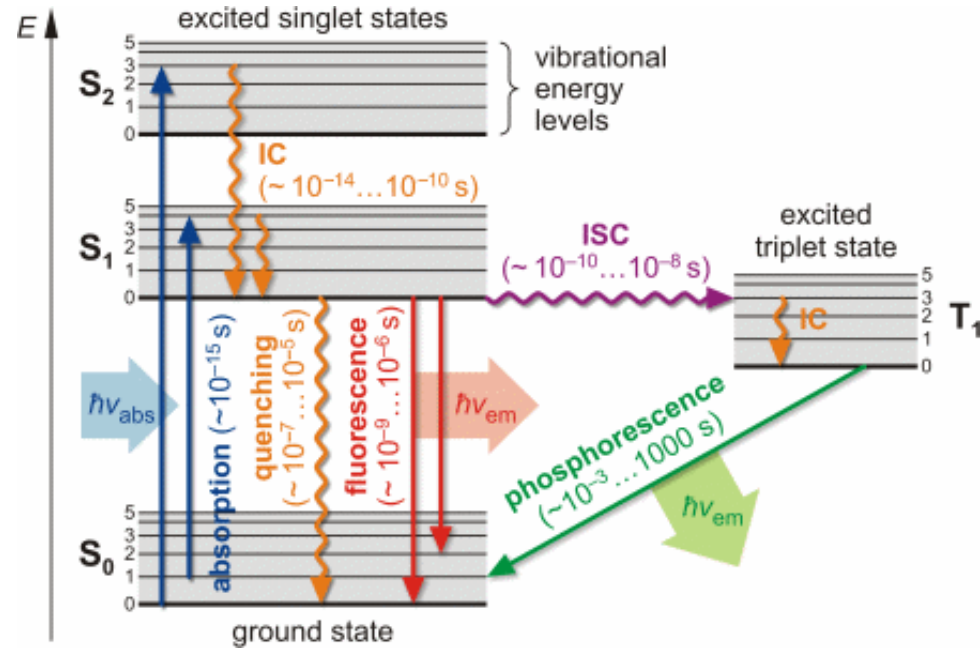
- Non-intrusive
- 2D measurements

Laser intensity & Tracer concentration variations?

- $I_1 = f(t) \rightarrow$ reference to normalize
- C depends on the local mixing

Multi-line approaches

- Two – color: independent to laser power and tracer concentration
 - Intensity ratio R_f of two different spectral bands



Signal



1-color: $I_f(\lambda) = K_{opt}(\lambda)K_{spec}(\lambda)V_d I_1 C e^{\beta(\lambda)/T}$

Intensity Ratio

2-color: $R_f(T) = \frac{I_{f,1}}{I_{f,2}} = \frac{K_{opt,1}}{K_{opt,2}} \exp\left(\frac{\beta_1 - \beta_2}{T}\right)$

LIF thermography

Choice of the technique

- Non-intrusive
- 2D measurements

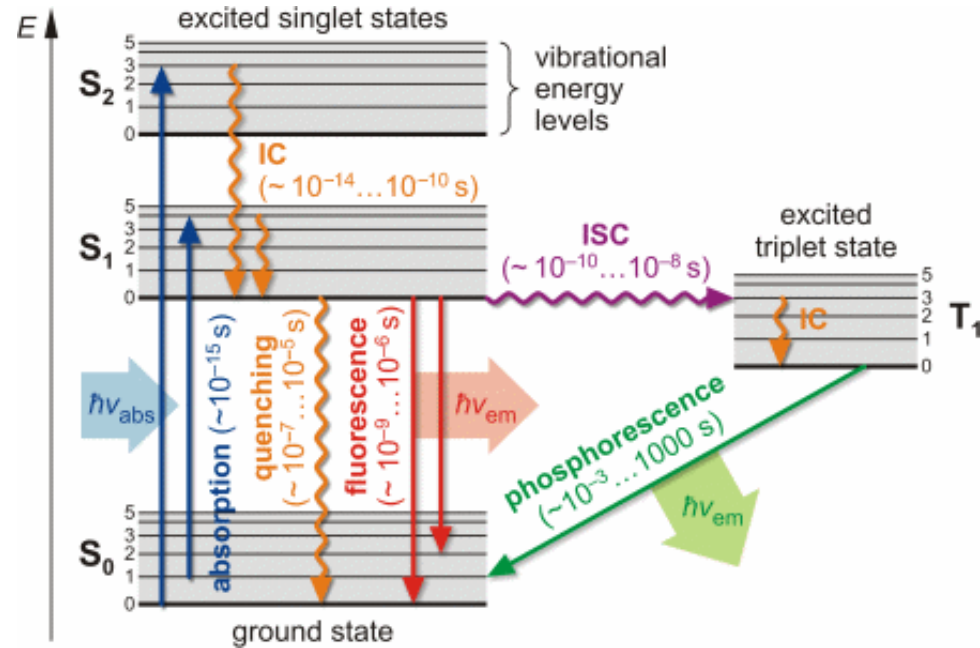
Laser intensity & Tracer concentration variations?

- $I_1 = f(t) \rightarrow$ reference to normalize
- C depends on the local mixing

Multi-line approaches

- Two – color: independent to laser power and tracer concentration
 - Intensity ratio R_f of two different spectral bands

Gas-phase LIF **tracer** (acetone or toluene)



Signal



$$1\text{-color: } I_f(\lambda) = K_{opt}(\lambda)K_{spec}(\lambda)V_d I_1 C e^{\beta(\lambda)/T}$$

Intensity Ratio

$$2\text{-color: } R_f(T) = \frac{I_{f,1}}{I_{f,2}} = \frac{K_{opt,1}}{K_{opt,2}} \exp\left(\frac{\beta_1 - \beta_2}{T}\right)$$

Mixture Prandtl number

NASA CEA (Equilibrium) algorithm
[McBride 1994] used with original
species

$$\square C_{p_{mix}} = \frac{\sum_{i=1}^N x_i C_{p_i}}{\sum_{i=1}^N x_i M_i}$$

$$\square \mu_{mix} = \sum_{i=1}^N \frac{x_i \mu_i}{x_i + \sum_{j=1}^N x_j \phi_{ij}}$$

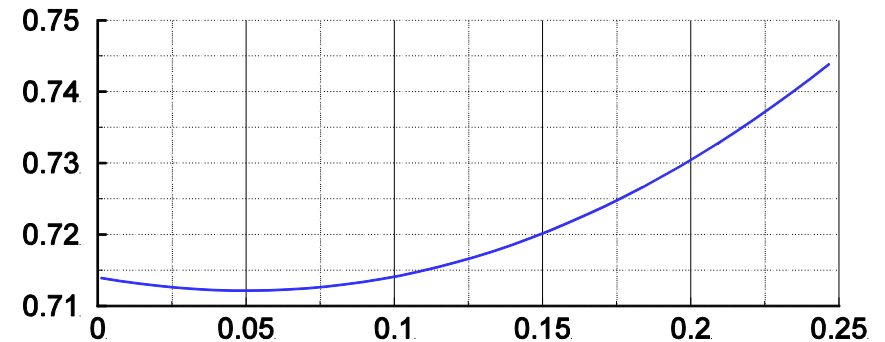
$$\square k_{mix} = \sum_{i=1}^N \frac{x_i k_i}{x_i + \sum_{j=1}^N x_j \psi_{ij}}$$

$$Pr_{mix} = \frac{C_{p_{mix}} \mu_{mix}}{k_{mix}}$$

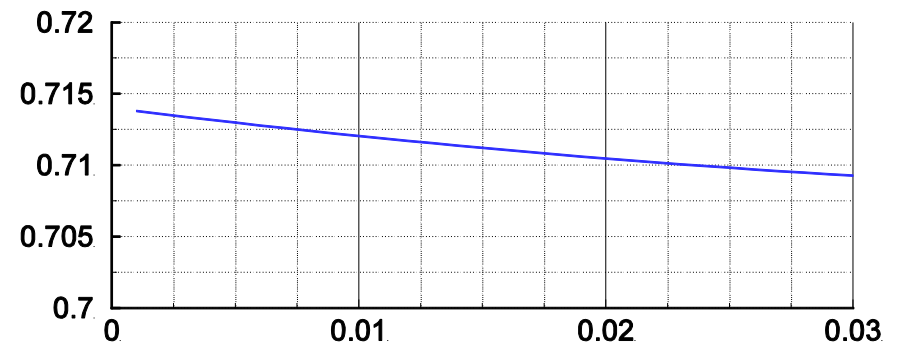
Pr_{mix}

Pr_{mix}

Acetone



Toluene



χ_{tracer}

χ_{tracer}

Mixture Prandtl number

NASA CEA (Equilibrium) algorithm
[McBride 1994] used with original
species

$$\square C_{p,mix} = \frac{\sum_{i=1}^N x_i C_{p,i}}{\sum_{i=1}^N x_i M_i}$$

$$\square \mu_{mix} = \sum_{i=1}^N \frac{x_i \mu_i}{x_i + \sum_{j=1}^N x_j \phi_{ij}}$$

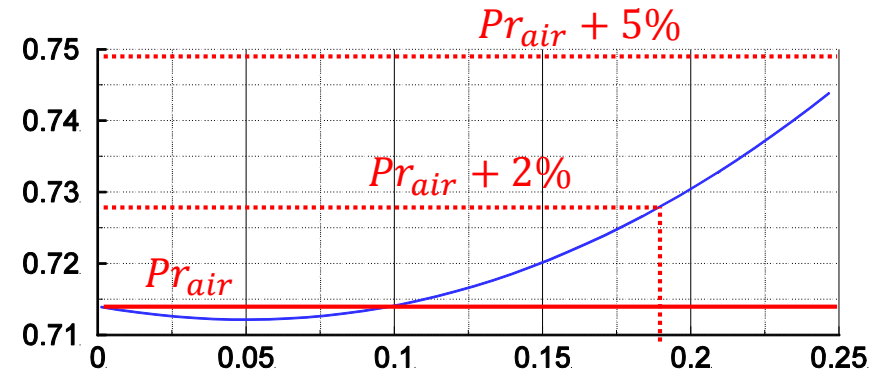
$$\square k_{mix} = \sum_{i=1}^N \frac{x_i k_i}{x_i + \sum_{j=1}^N x_j \psi_{ij}}$$

$$Pr_{mix} = \frac{C_{p,mix} \mu_{mix}}{k_{mix}}$$

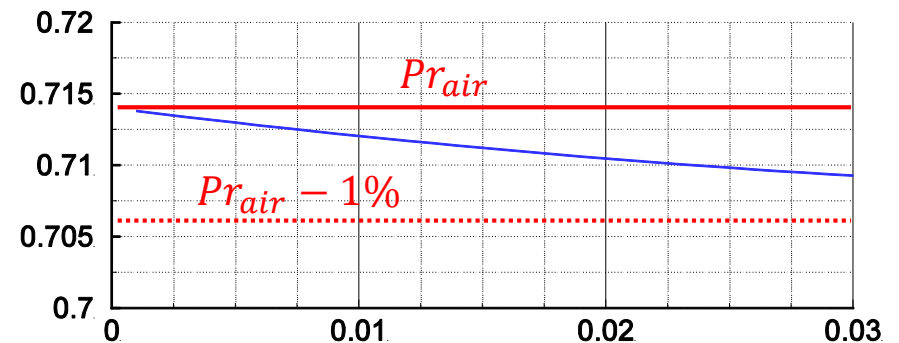
Pr_{mix}

Pr_{mix}

Acetone



Toluene

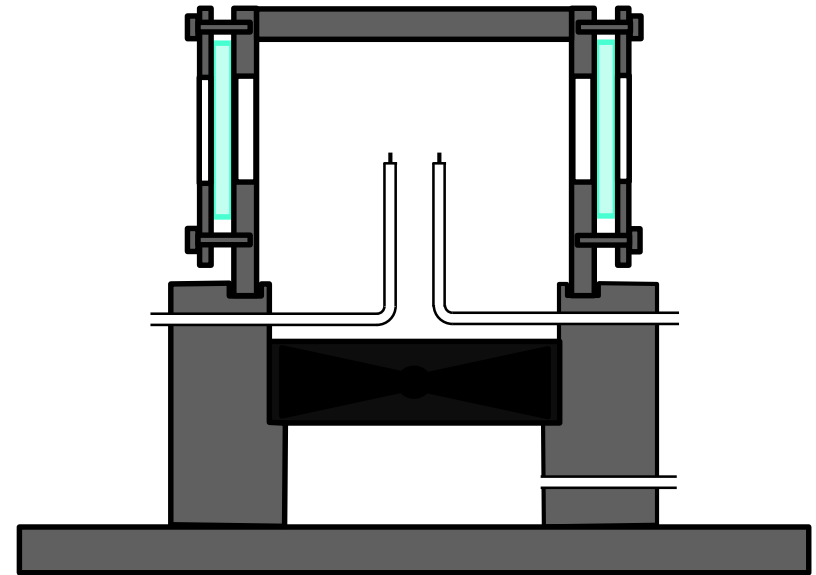


X_{tracer}

X_{tracer}

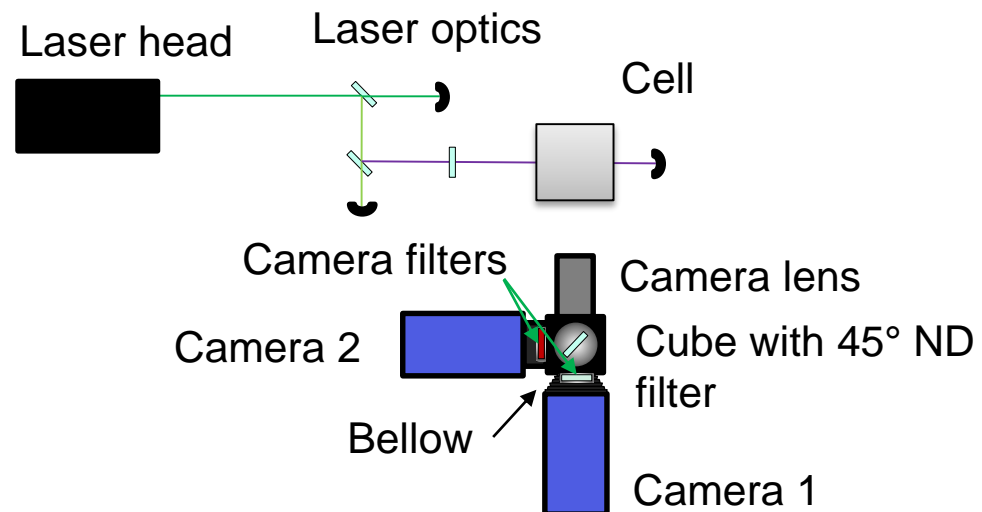
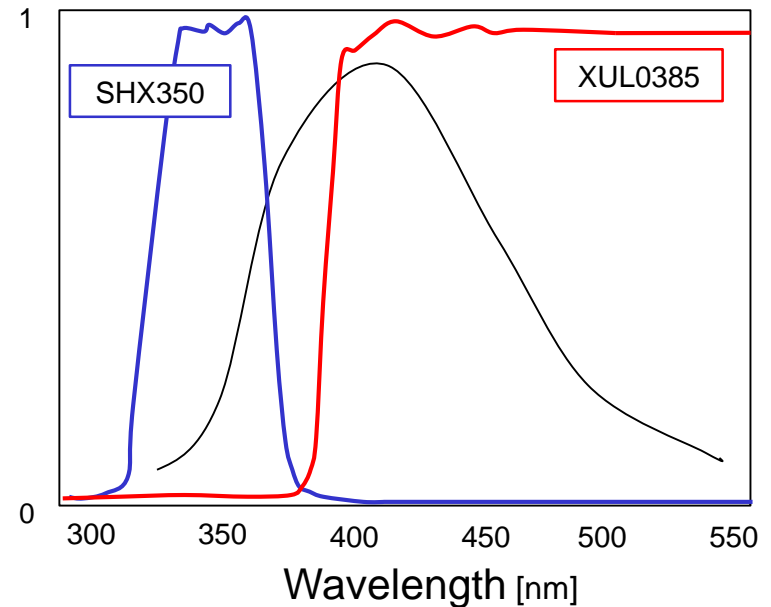
Measurement cell

- ❑ 50x50x90 mm^3 aluminum cell
- ❑ Optical accesses with quartz plates (laser + cameras)
- ❑ Temperature control and acquisition by 4 thermocouples
- ❑ Tracer access
- ❑ Mixing by a fan
- ❑ Heated from the bottom (heat gun)

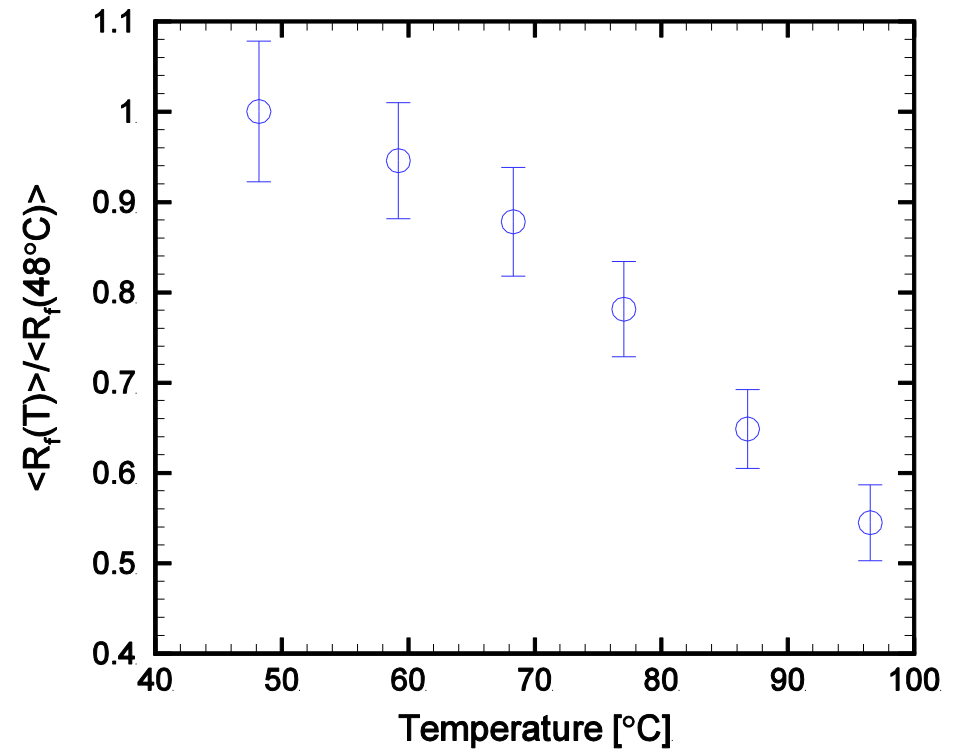


Two-color acetone measurements

- ❑ Selection of the two bandwidths based on VKI's spectral measurements
- ❑ Experimental set-up
 - UV-laser (266nm and 532nm)
 - Laser optics (2 dichroic mirrors + spherical lens)
 - Measurement cell
 - 2 perpendicular cameras
 - 2 band-pass filters
 - ND filter at 45°
 - Camera lens (100mm fused-silica spherical lens)
 - Air-acetone vapor mixture

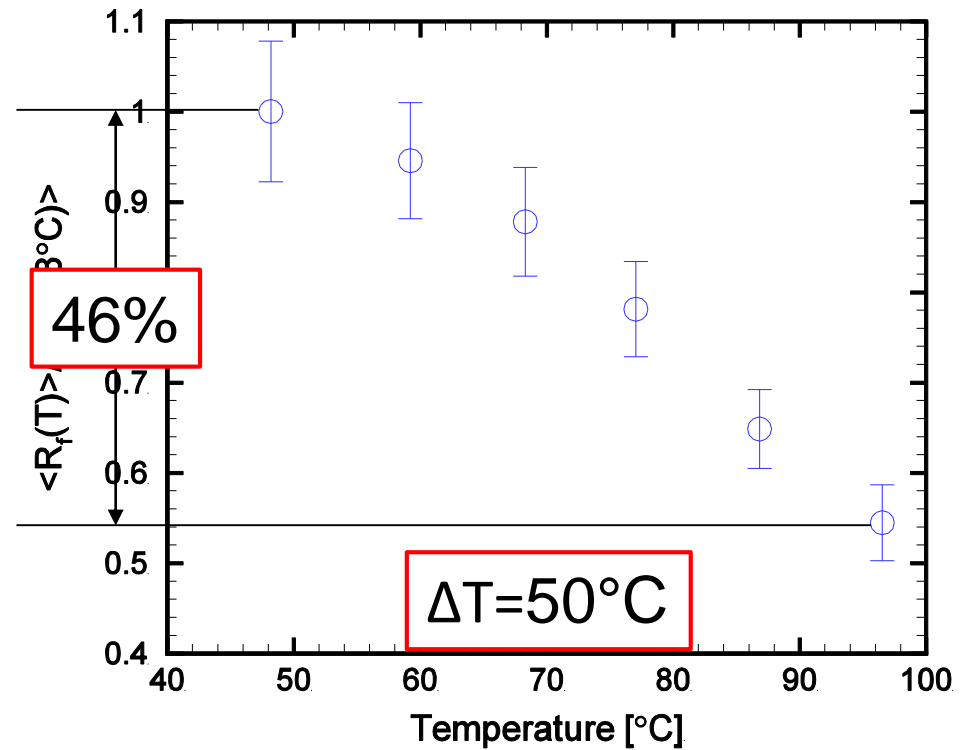


Results and Conclusions



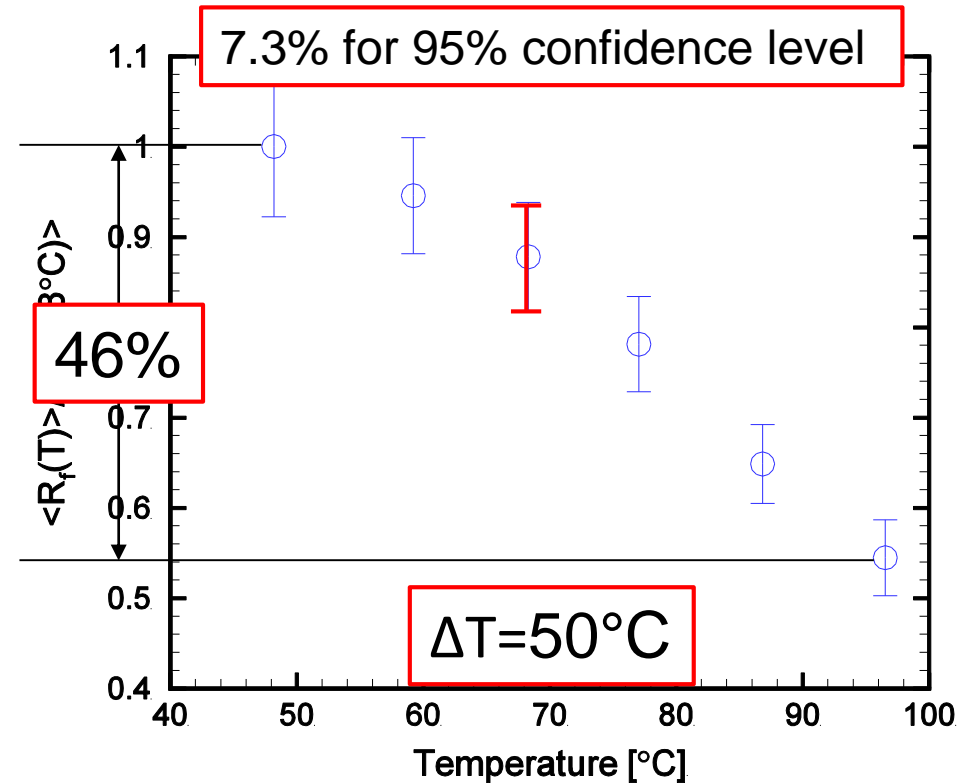
Results and Conclusions

- 46% decrease corresponding to 50°C temperature difference



Results and Conclusions

- ❑ 46% decrease corresponding to 50°C temperature difference
- ❑ Uncertainty of 7.3% for 95% confidence level $\Rightarrow \pm 8^\circ\text{C}$

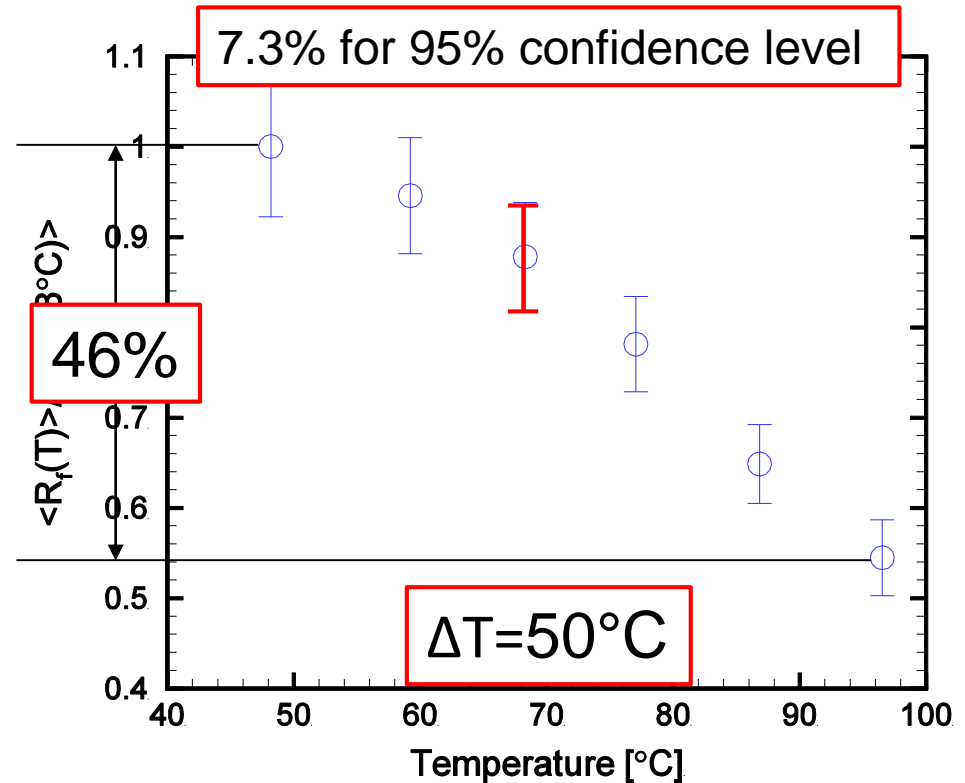


Results and Conclusions

- ❑ 46% decrease corresponding to 50°C temperature difference
- ❑ Uncertainty of 7.3% for 95% confidence level $\Rightarrow \pm 8^\circ\text{C}$

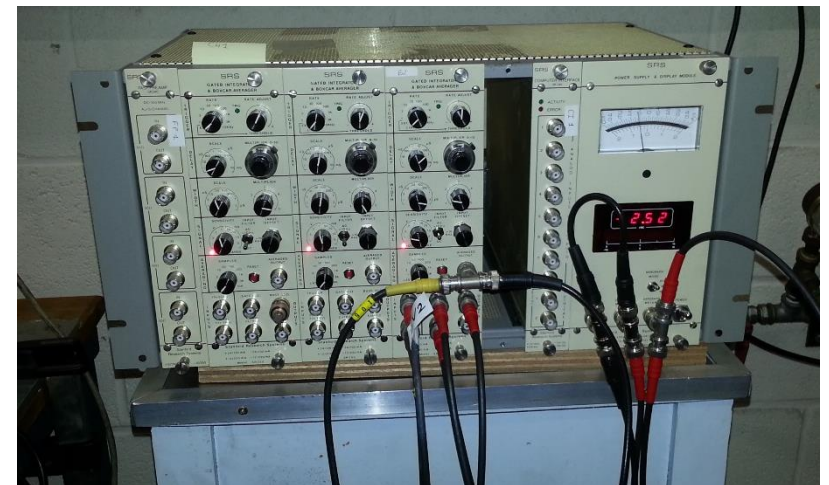
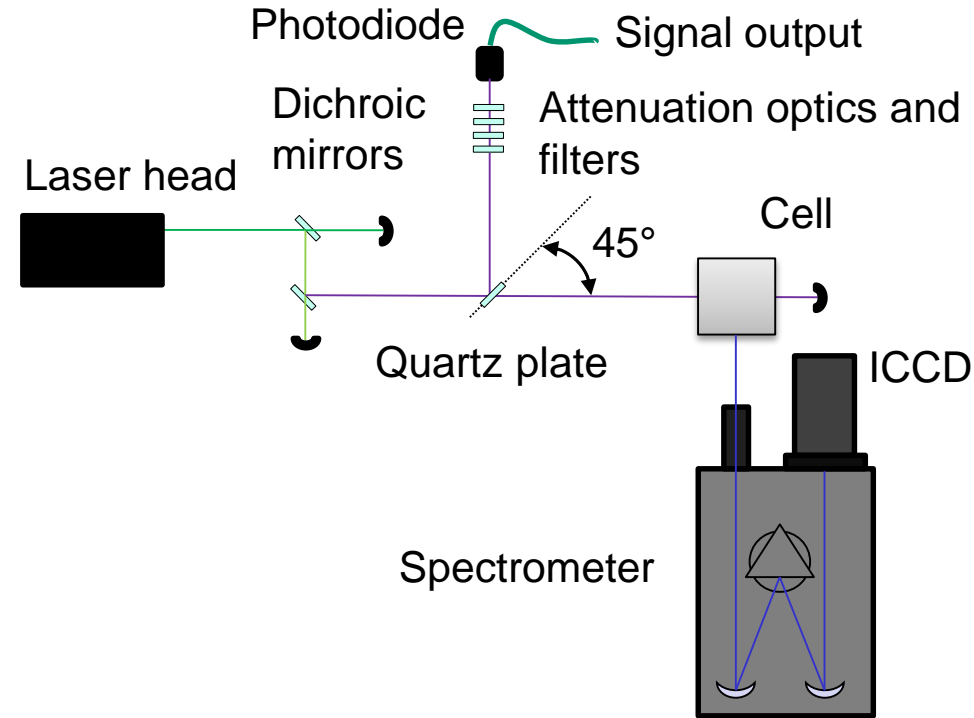


- ❑ Encouraging dependence of R_f with temperature but:
 - Low signal \Rightarrow high uncertainty
 - No evidence in literature (no two-color acetone studies)
- ❑ Spectral measurements of acetone fluorescence



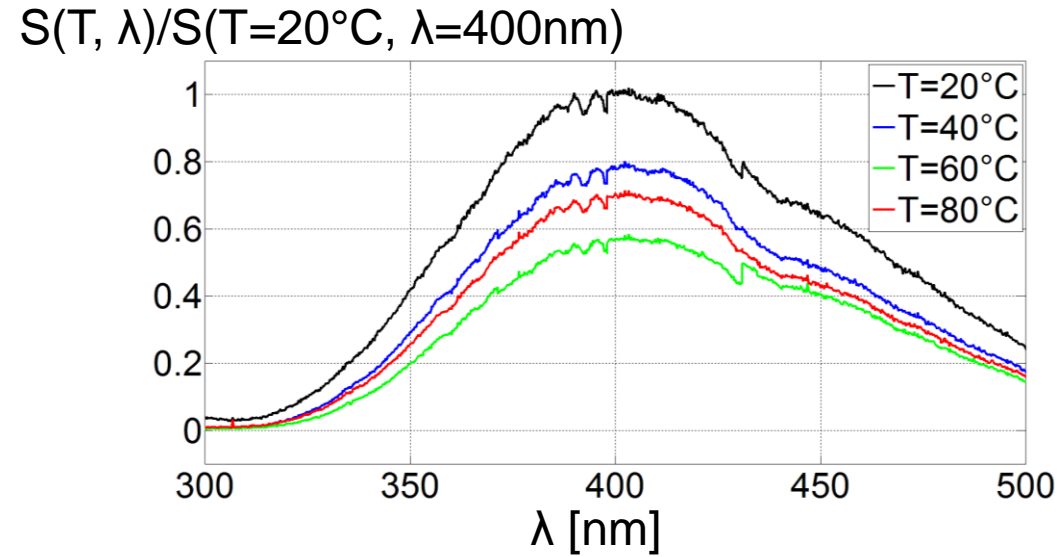
Acetone Spectral Measurement

- ❑ Spectrometer + ICCD camera
- ❑ Laser energy reference measurement by photodiode
 - Quartz plate at 45° reflect 1÷5% light at 90°
 - Optics attenuate light and cut down the green component
 - Photodiode produces signal \propto light intensity
 - Signal integrated by a Box Averager and sent to the acquisition system



Results and Conclusions

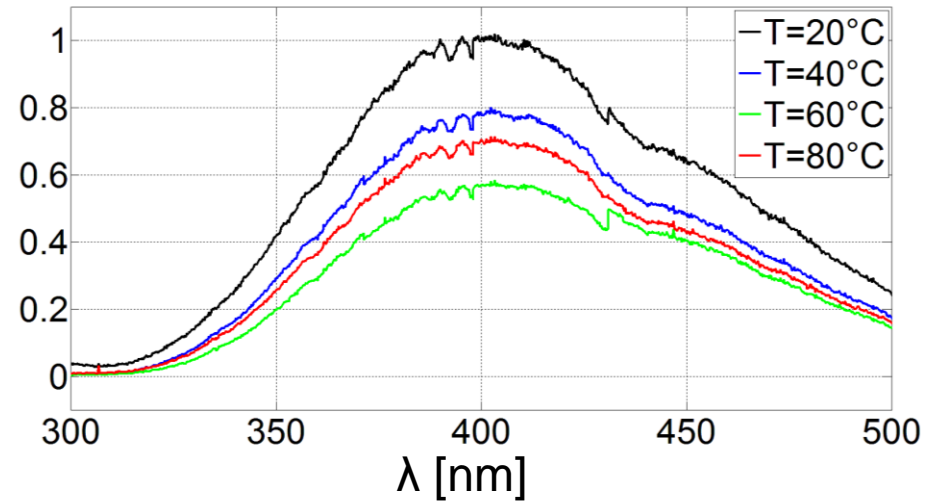
- Clear dependence of the signal with temperature



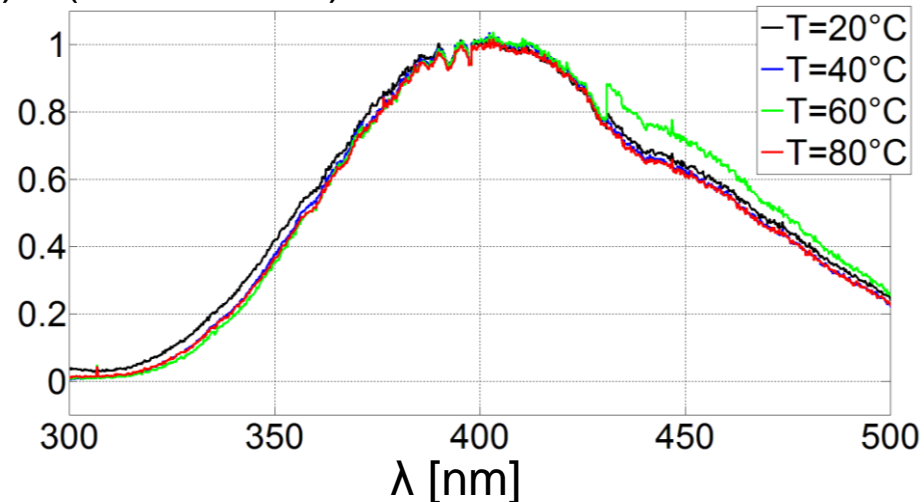
Results and Conclusions

- ❑ Clear dependence of the signal with temperature
- ❑ Not appreciable red shift or shape change
- ❑ Theoretically two-color technique not possible with acetone

$$S(T, \lambda)/S(T=20^\circ\text{C}, \lambda=400\text{nm})$$



$$S(T, \lambda)/S(T, \lambda=400\text{nm})$$



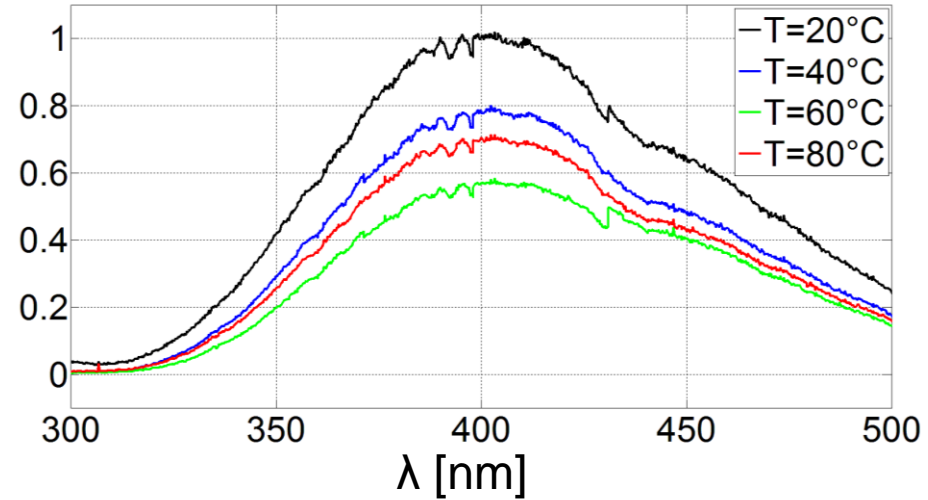
Results and Conclusions

- ❑ Clear dependence of the signal with temperature
- ❑ Not appreciable red shift or shape change
- ❑ Theoretically two-color technique not possible with acetone

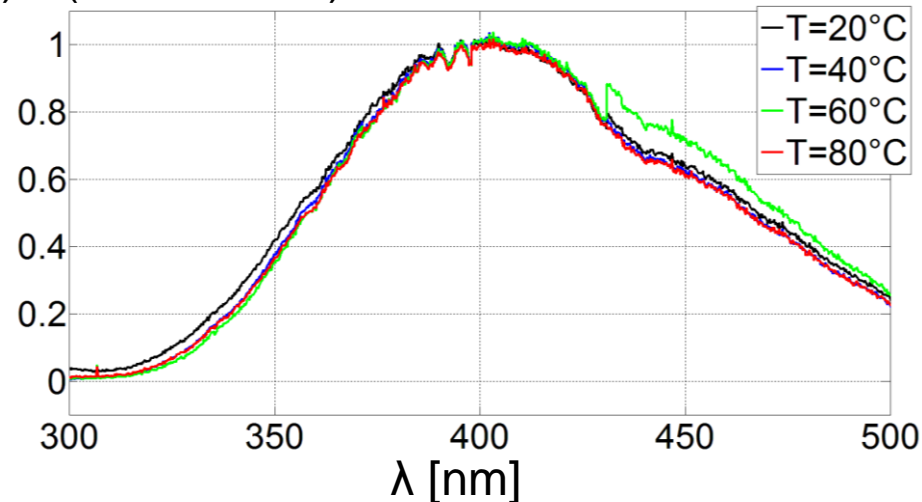


- ❑ Other phenomena we do not take into account
- ❑ Other tracer (toluene or anisole) or one-color technique
- ❑ Need of testing in a continuous flow (2D internal flow)

$S(T, \lambda)/S(T=20^\circ\text{C}, \lambda=400\text{nm})$

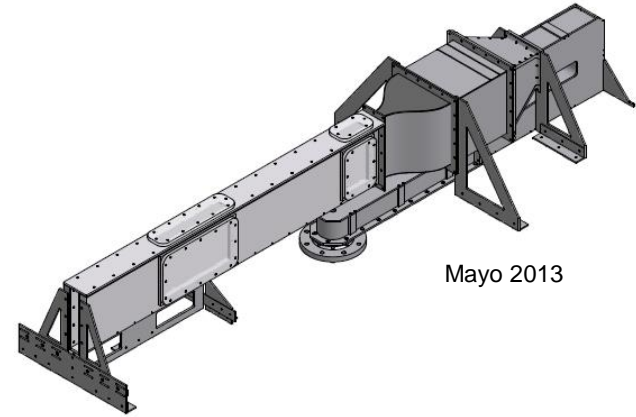


$S(T, \lambda)/S(T, \lambda=400\text{nm})$



Facility

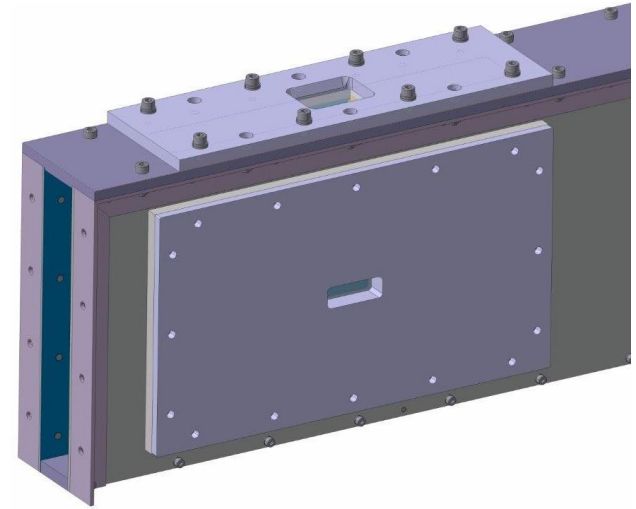
- ❑ Existing aluminum channel
 - with high aspect ratio ($W/H = 6$)



Mayo 2013

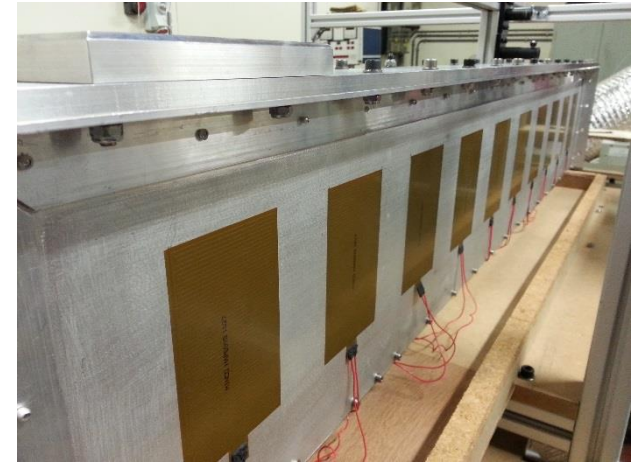
Facility

- ❑ Existing aluminum channel
 - with high aspect ratio ($W/H = 6$)
 - re-designed optical accesses



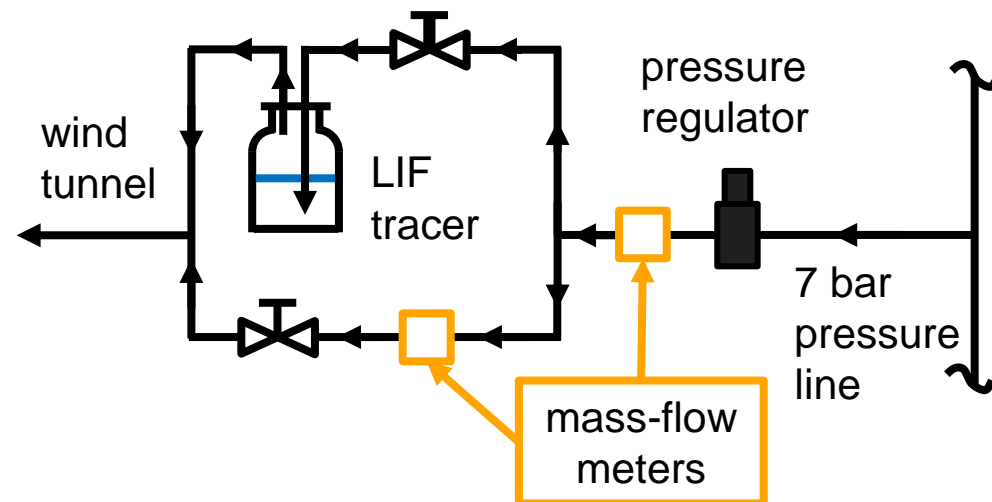
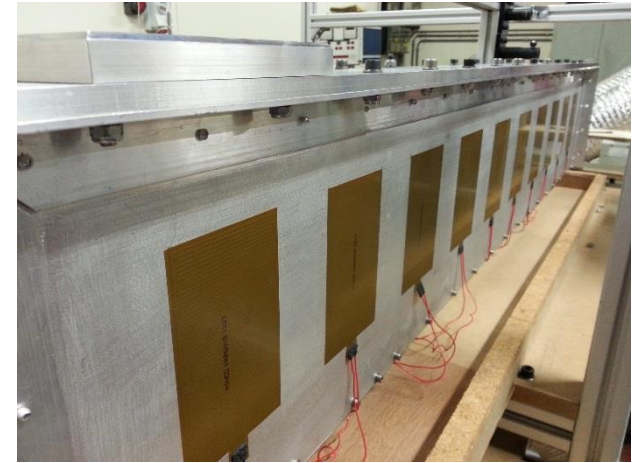
Facility

- ❑ Existing aluminum channel
 - with high aspect ratio ($W/H = 6$)
 - re-designed optical accesses
 - Heated bottom wall with thin resistances



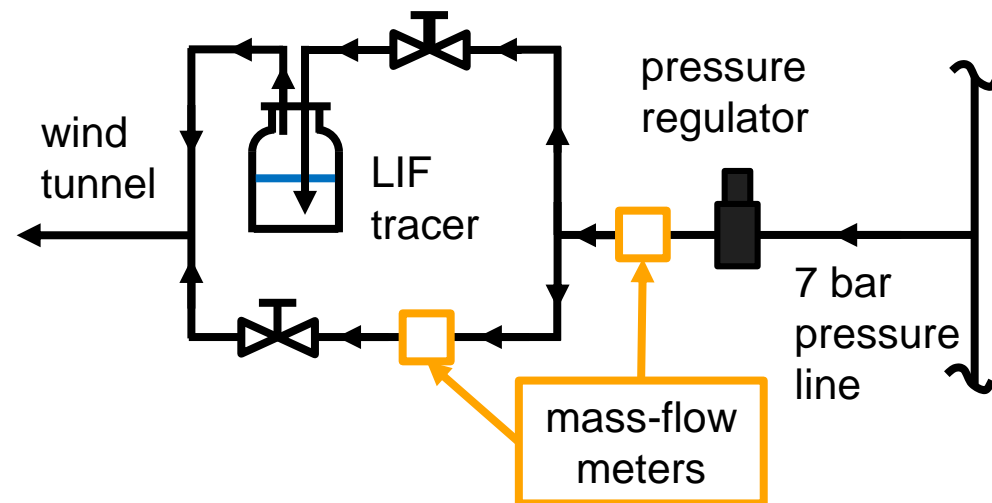
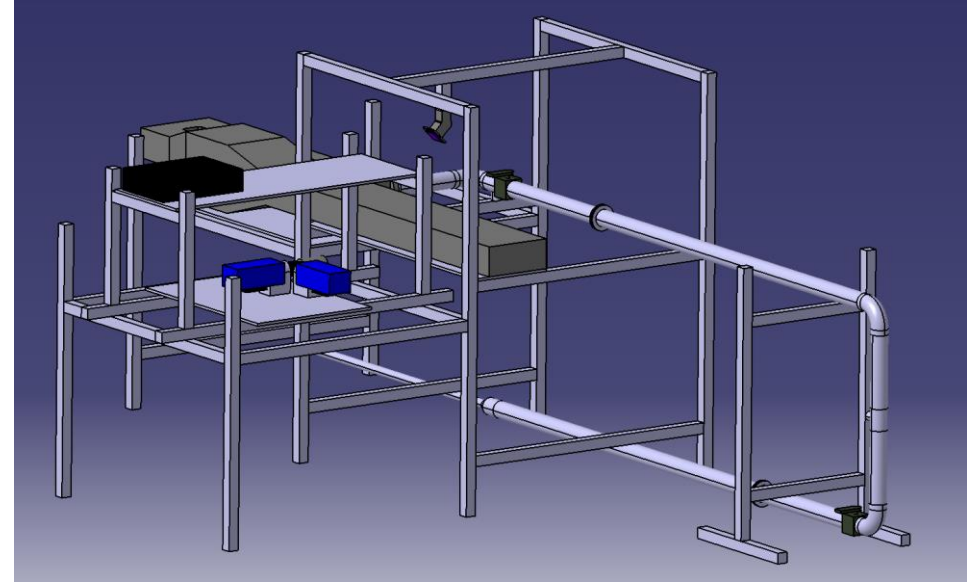
Facility

- ❑ Existing aluminum channel
 - with high aspect ratio ($W/H = 6$)
 - re-designed optical accesses
 - Heated bottom wall with thin resistances
- ❑ Piping of PE100 DN50 mm:
 - Seeding air with fluorescent tracer
 - Control mass-flow and tracer concentration with two orifice plates
 - extraction



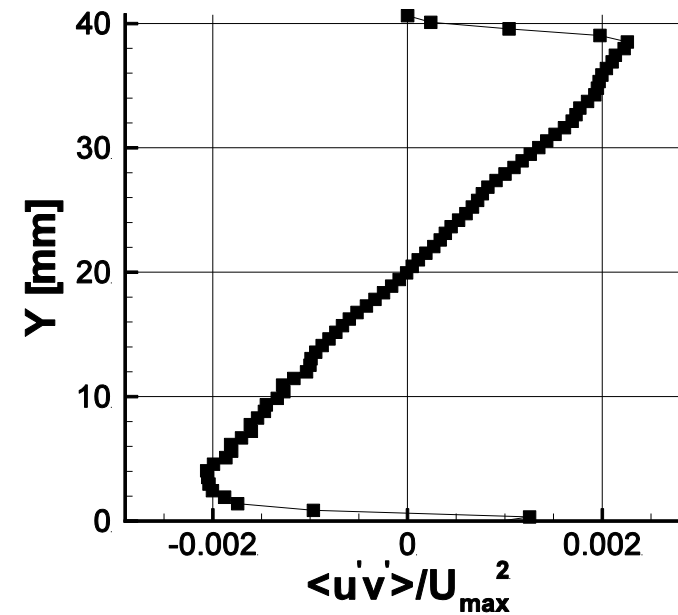
Facility

- ❑ Existing aluminum channel
 - with high aspect ratio ($W/H = 6$)
 - re-designed optical accesses
 - Heated bottom wall with thin resistances
- ❑ Piping of PE100 DN50 mm:
 - Seeding air with fluorescent tracer
 - Control mass-flow and tracer concentration with two orifice plates
 - extraction
- ❑ Supports (aluminum profiles and corners)
- ❑ Instrumentation (Laser and cameras)



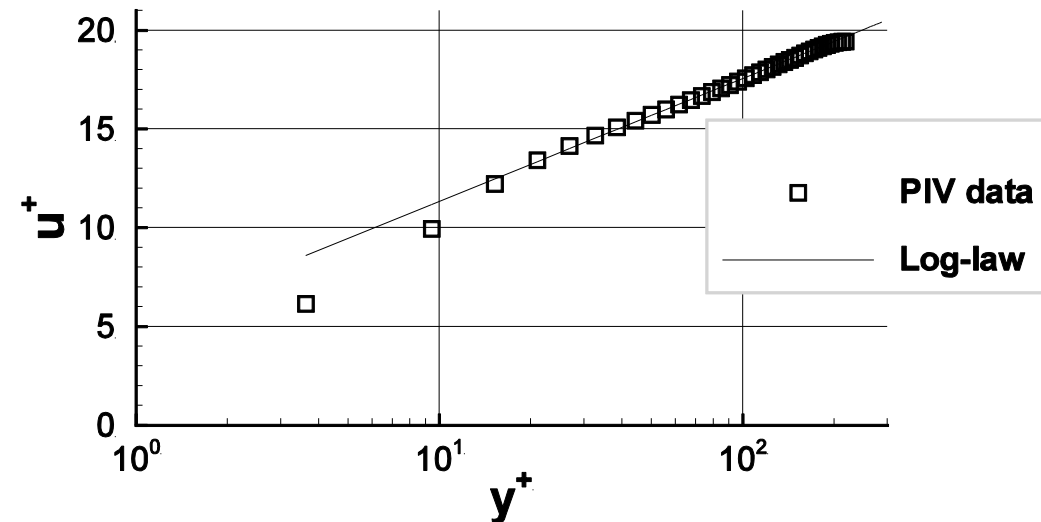
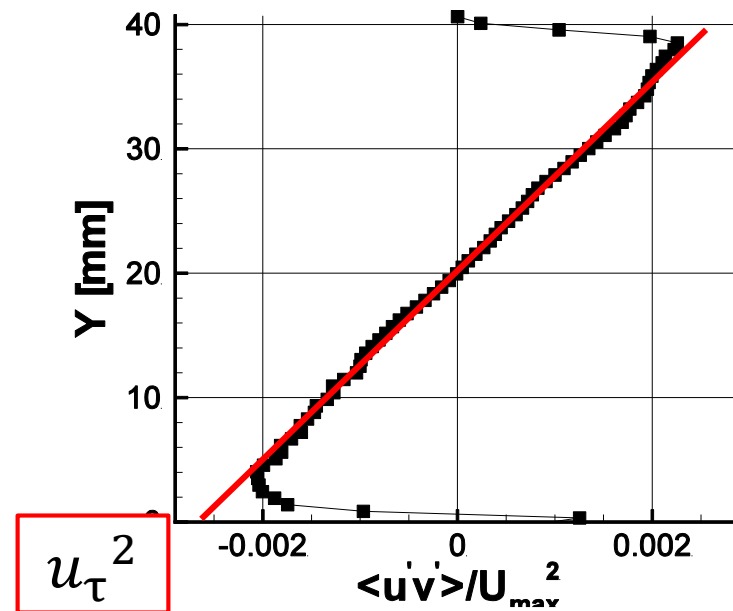
Flow characterization with PIV

- Fully turbulent and fully developed velocity profile at $Re_H = 6700$
- Reynolds stresses for the determination of u_τ , u^+ and y^+



Velocity profile with PIV

- Fully turbulent and fully developed velocity profile at $Re_H = 6700$
- Reynolds stresses for the determination of u_τ , u^+ and y^+
- Match of the logarithmic law ($\kappa = 0.37$, $B = 5.1$)



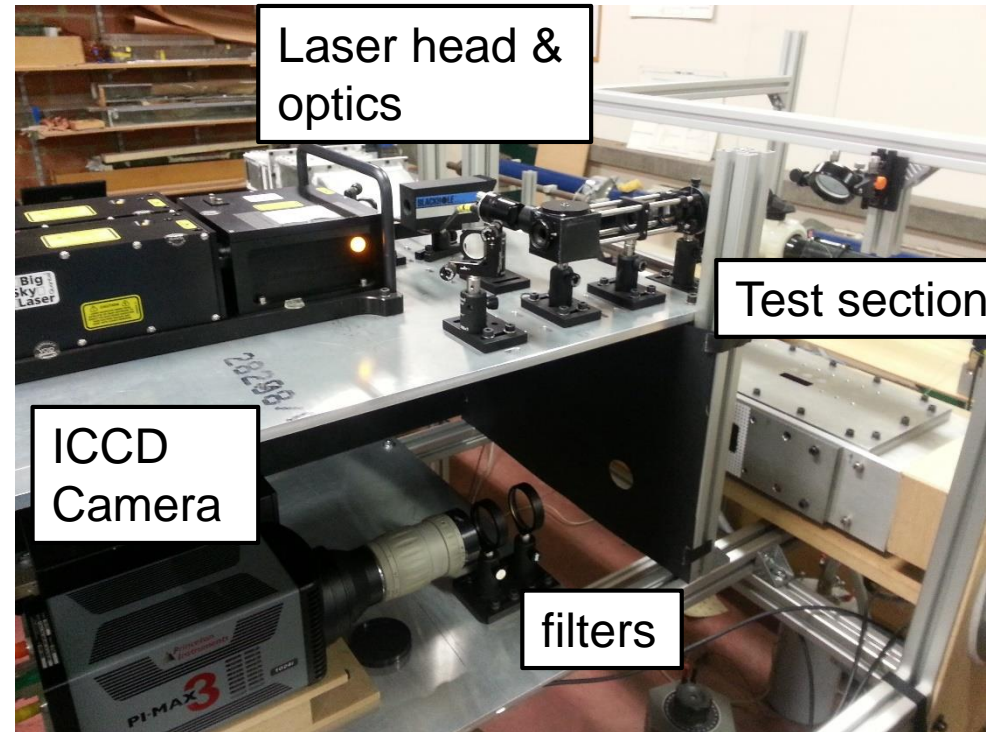
Air-Toluene LIF measurements

❑ Experimental set-up

- Laser and optics (as in spectral measurements) + mirror
- ICCD camera provided by Semrock Razor Edge 266nm and 400 nm Low pass filters

❑ Methodology

- 10 images of a dotted plate (spatial calibration)
- 10 images of background BG
- 100 images of fluorescence at isothermal conditions I_{AMB} (Flat Field)
- 100 images of fluorescence with the bottom wall heated around 70°C I_{HW}



$$I^* = \frac{I_{HW} - \overline{BG}}{I_{AMB} - \overline{BG}}$$

Results and conclusions

- ❑ Traverse measurements with a type-K thermocouple probe

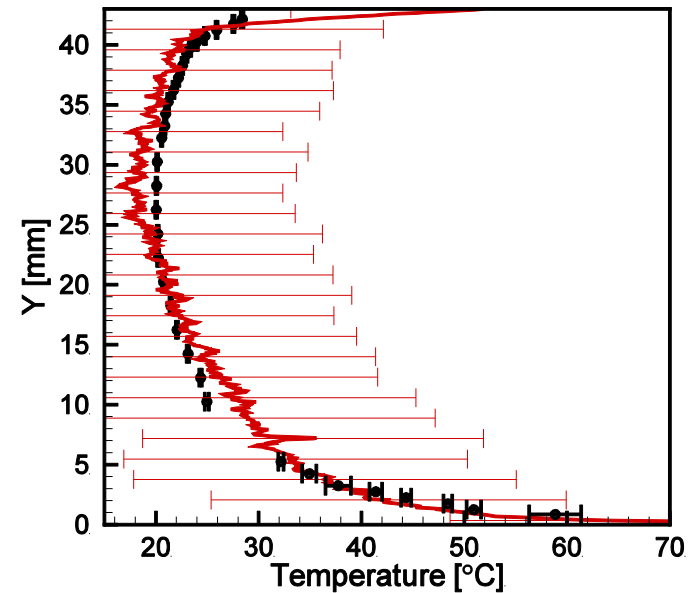


Results and conclusions

- ❑ Traverse measurements with a type-K thermocouple probe
- ❑ Two-points temperature calibration with linear function

$$T = a + b * I^*$$

- ❑ Comparison of the averaged I^* (red line) with the thermocouple output (black circles)



Results and conclusions

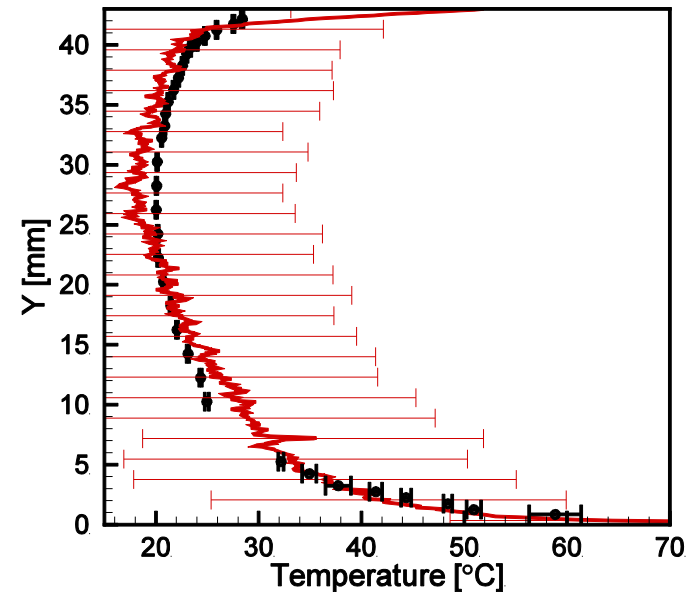
- ❑ Traverse measurements with a type-K thermocouple probe
- ❑ Two-points temperature calibration with linear function

$$T = a + b * I^*$$

- ❑ Comparison of the averaged I^* (red line) with the thermocouple output (black circles)



- ❑ Good match of the temperature profiles with missing points
- ❑ Uncertainty of 10% $\Rightarrow \pm 12^\circ\text{C}$



Results and conclusions

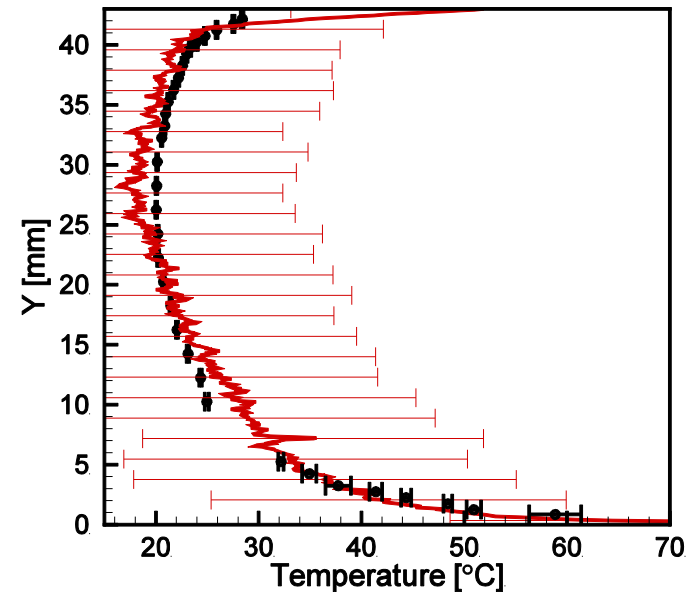
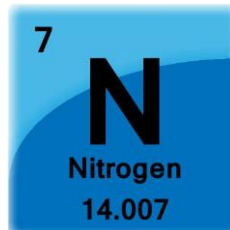
- ❑ Traverse measurements with a type-K thermocouple probe
- ❑ Two-points temperature calibration with linear function

$$T = a + b * I^*$$

- ❑ Comparison of the averaged I^* (red line) with the thermocouple output (black circles)



- ❑ Good match of the temperature profiles with missing points
- ❑ Uncertainty of 10% $\Rightarrow \pm 12^\circ\text{C}$
 \Rightarrow blow nitrogen



Nitrogen-Toluene LIF measurements

- Higher signal (20 times higher with no oxygen content)

⇒ higher S/N ratio ⇒ lower δI^*

$$\delta T \approx \delta I^* \cdot \frac{\Delta T}{\Delta I^*}$$

Nitrogen-Toluene LIF measurements

- Higher signal (20 times higher with no oxygen content)

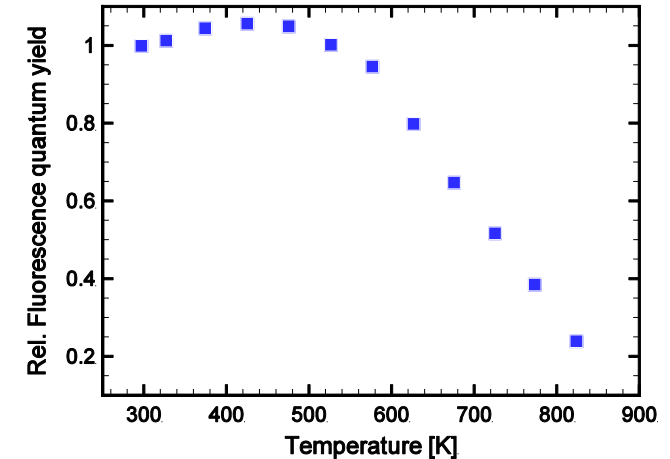
⇒ higher S/N ratio ⇒ lower δI^*

- Higher temperature dependence $\frac{\Delta I^*}{\Delta T}$

⇒ lower $\frac{\Delta T}{\Delta I^*}$

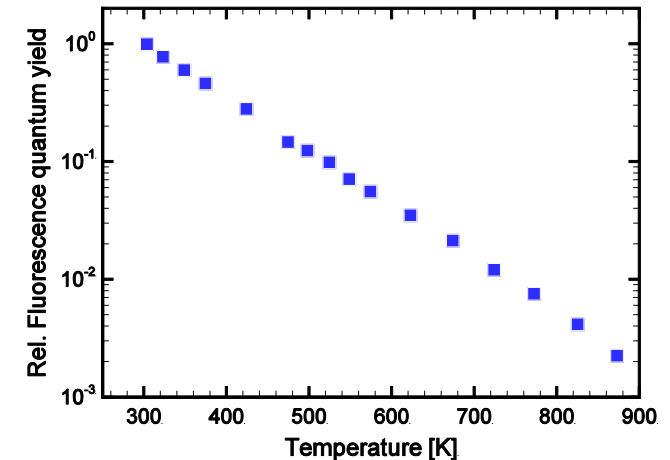
$$\delta T \approx \delta I^* \cdot \frac{\Delta T}{\Delta I^*}$$

Air



Faust 2013

N2



Faust 2013

Nitrogen-Toluene LIF measurements

- ❑ Higher signal (20 times higher with no oxygen content)

⇒ higher S/N ratio ⇒ lower δI^*

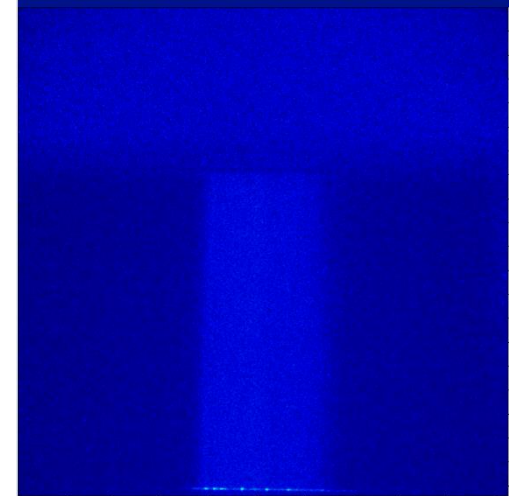
- ❑ Higher temperature dependence $\frac{\Delta I^*}{\Delta T}$

⇒ lower $\frac{\Delta T}{\Delta I^*}$

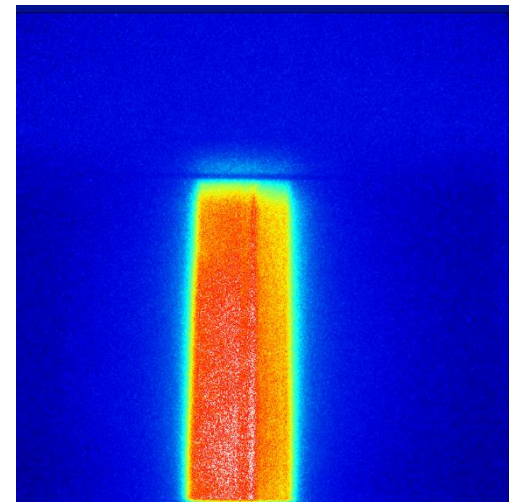
$$\delta T \approx \delta I^* \cdot \frac{\Delta T}{\Delta I^*}$$

- ❑ Measured signal 10 times higher
- ❑ Decrease of camera noise from 13% to 8%

Air

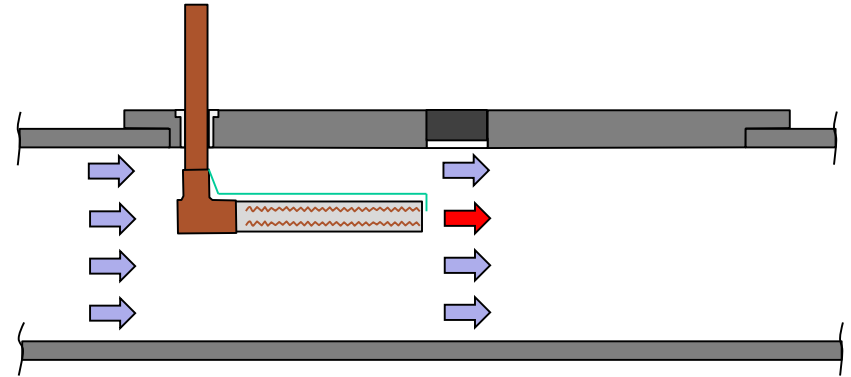


N2



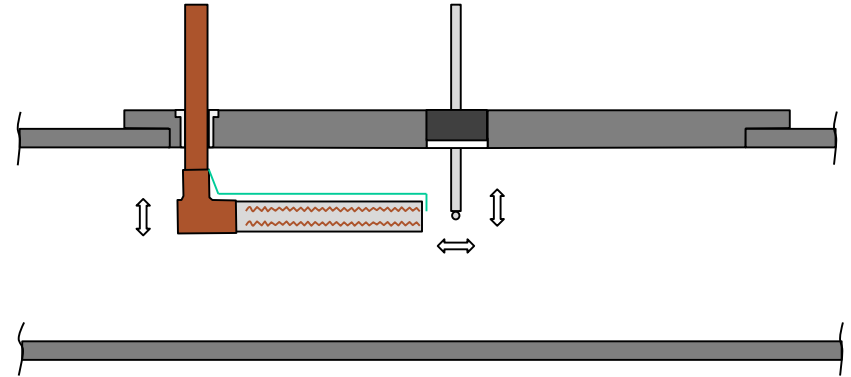
Temperature calibration

- In-situ calibration
- Flow temperature increased by a heater
- Thermocouple at the exit to control the operating conditions



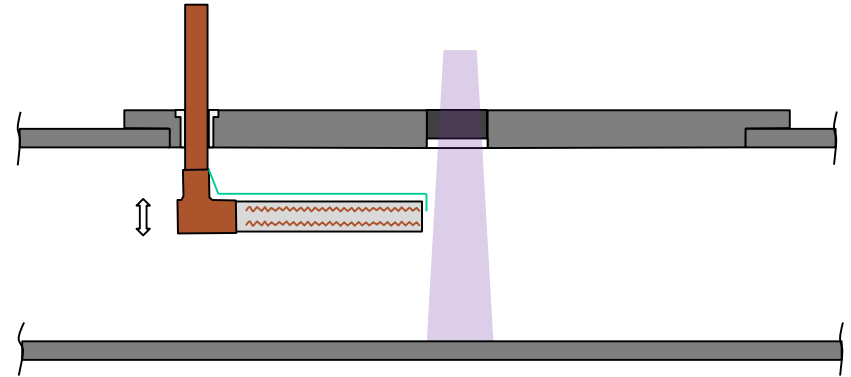
Temperature calibration

- ❑ In-situ calibration
- ❑ Flow temperature increased by a heater
- ❑ Thermocouple at the exit to control the operating conditions
- ❑ Calibration Methodology:
 - Heater & Thermocouple probe at 4 different positions along the channel height and the thermocouple at 3 different horizontal positions



Temperature calibration

- ❑ In-situ calibration
- ❑ Flow temperature increased by a heater
- ❑ Thermocouple at the exit to control the operating conditions
- ❑ Calibration Methodology:
 - Heater & Thermocouple probe at 4 different positions along the channel height and the thermocouple at 3 different horizontal positions
 - Heater & LIF laser sheet at different positions along the channel height



Conclusions and Future Work

- ❑ Innovative information by addressing **Flow Temperature Data**
- ❑ Preliminary results are encouraging
- ❑ Design of a novel Facility
- ❑ Flow characterization
- ❑ Match of the temperature profile with air-toluene one-color LIF
- ❑ Nitrogen-toluene one-color LIF upgrade with significant decrease of noise

Conclusions and Future Work

- ❑ Innovative information by addressing **Flow Temperature Data**
- ❑ Preliminary results are encouraging
- ❑ Design of a novel Facility
- ❑ Flow characterization
- ❑ Match of the temperature profile with air-toluene one-color LIF
- ❑ Nitrogen-toluene one-color LIF upgrade with significant decrease of noise

- ❑ Nitrogen measurements
- ❑ Apply the in-situ calibration designed
- ❑ Further analysis (e.g. temperature fluctuations)
- ❑ PIV/LIF set-up $\Rightarrow \overline{v'T'}$ and Pr_t
- ❑ Application of ribbed channel

UCL

Université
catholique
de Louvain

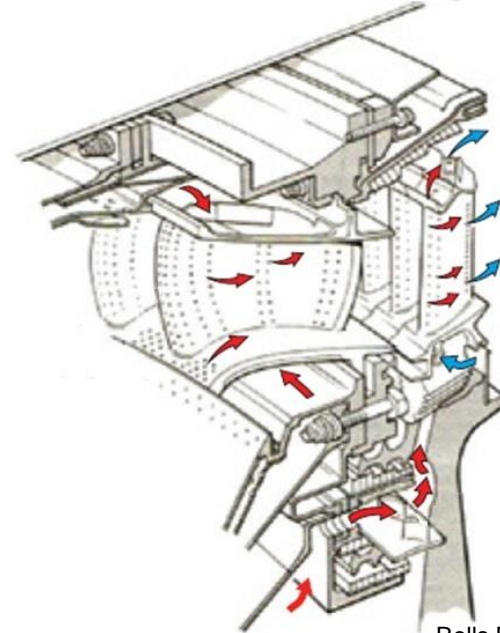
fnrs
LA LIBERTÉ DE CHERCHER



LIF Temperature field Measurements for Internal Forced Convection Blade Cooling

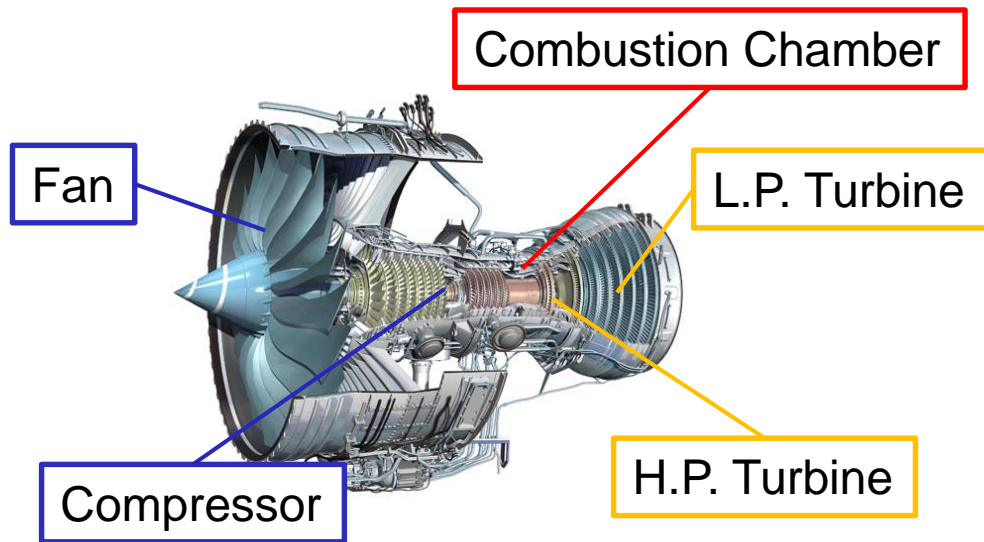
Gian Luca Gori

Supervisor: Tony Arts



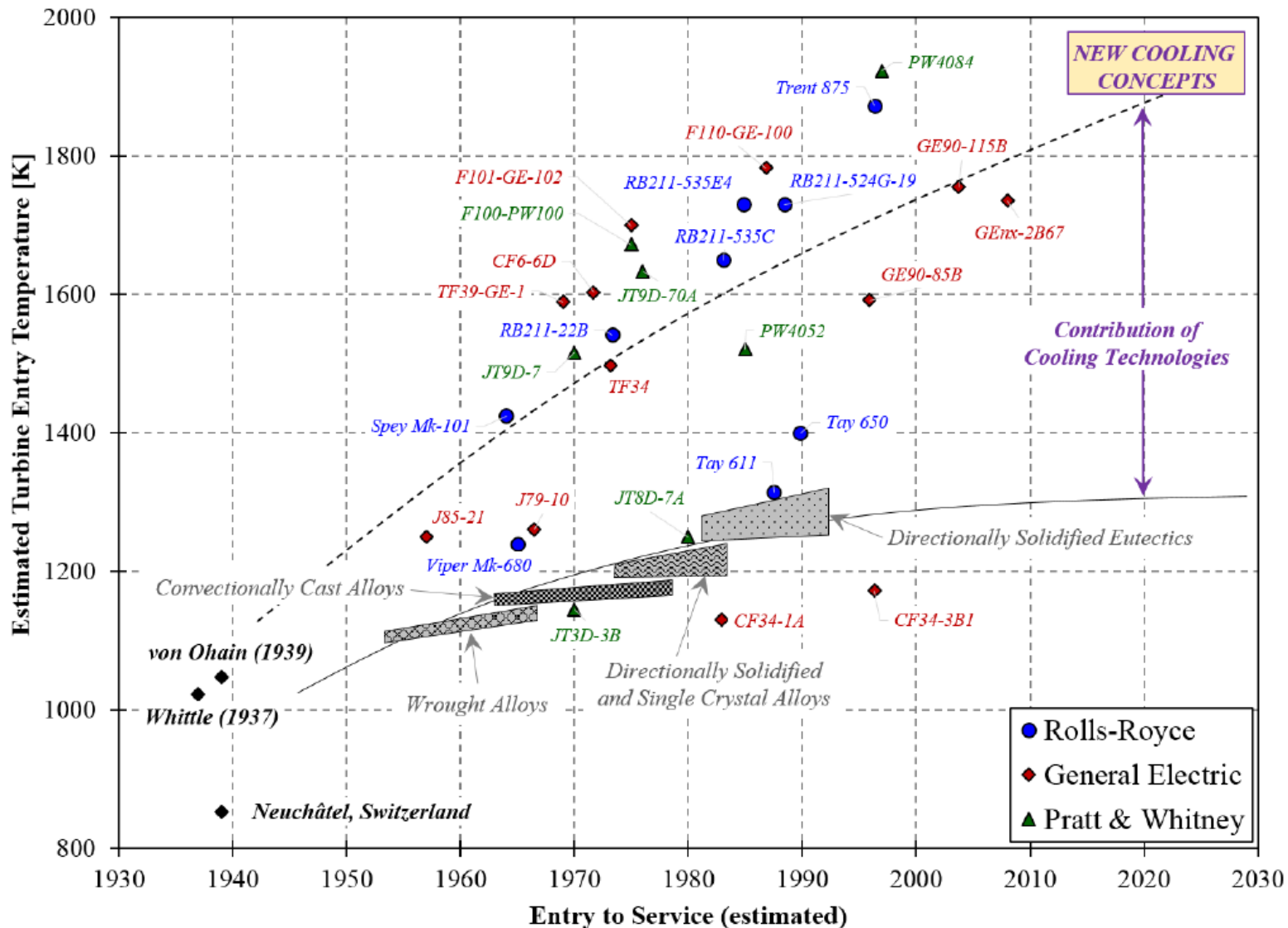
Rolls Royce - The Jet Engine

Rolls Royce Trent 1000

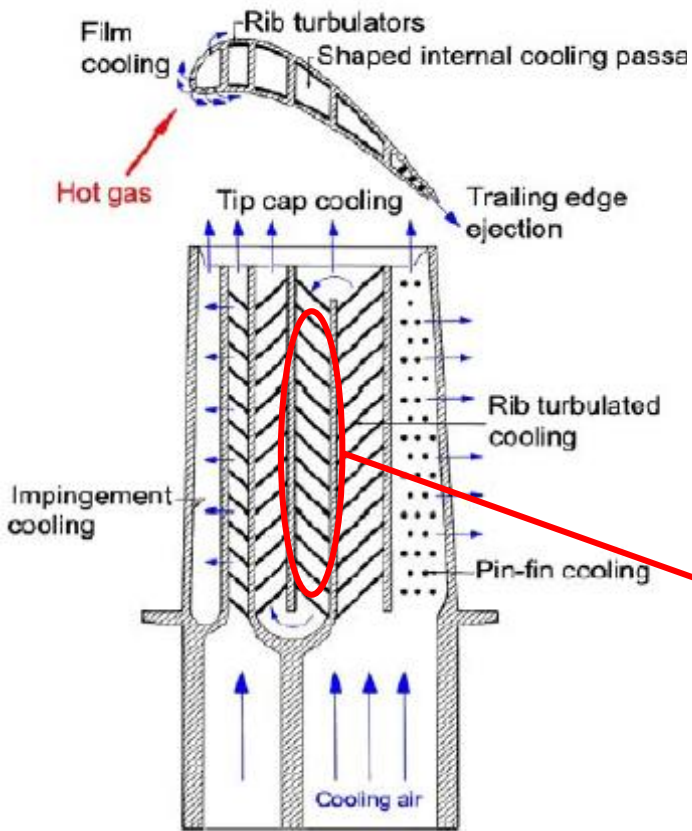


Application	Boeing 787
By-pass Ratio	(10.8÷11):1
Length	4.74 m
Diameter	2.85 m
Dry Weight	5,765 kg
Compressor	1LP,8IP,6HP
Combustor	Tiled
Turbine	1HP,1IP,6LP
Maximum Thrust	276÷376 kN
Pressure Ratio	52:1
Air mass-flow	1,290 kg/s
Thrust/Weight	6.189:1

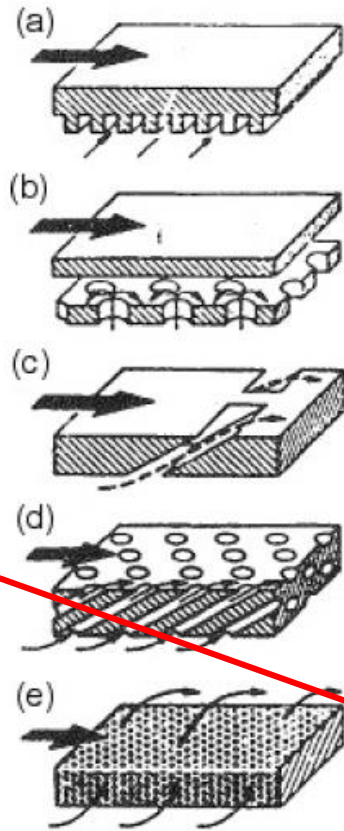
TIT evolution



Cooling Techniques



Han, 2004



Lozza, 2006

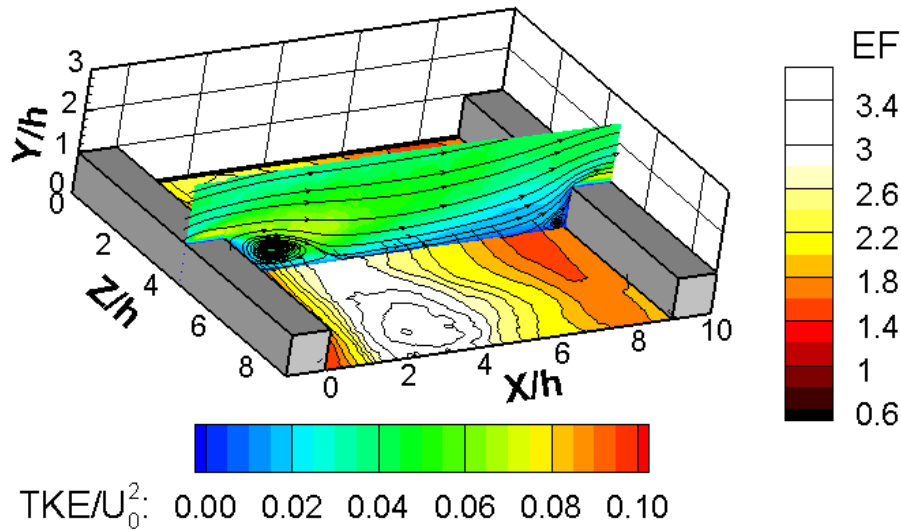
- (a) forced convection
- (b) impingement
- (c,d) film
- (e) transpiration

Internal Cooling Channel

Project Profits

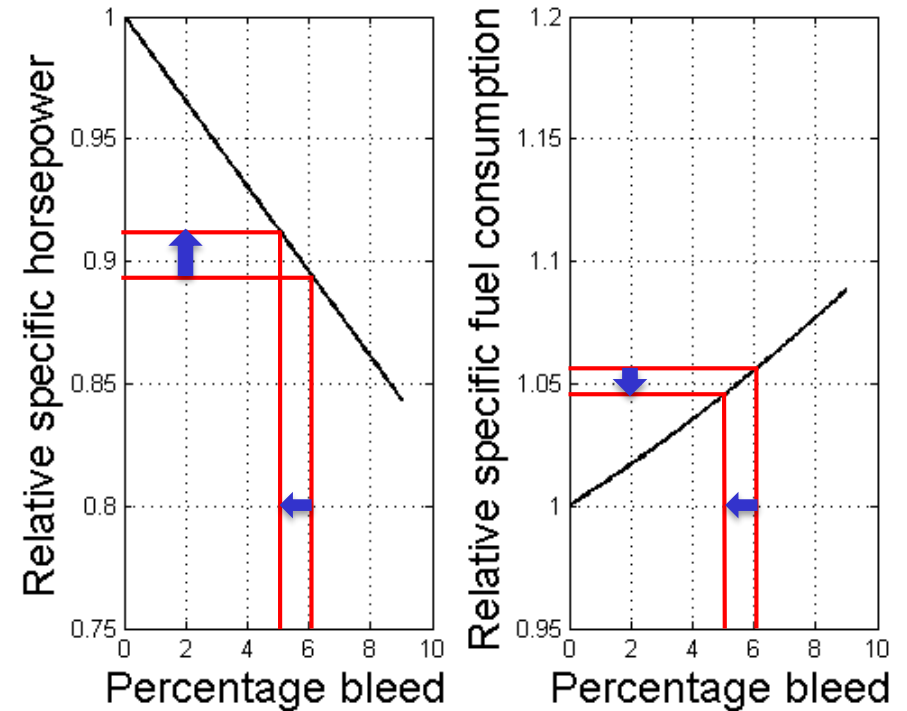
Fundamental improvements

- Understanding of the Physics
- Modeling & Validation
 - Aero
 - Thermal



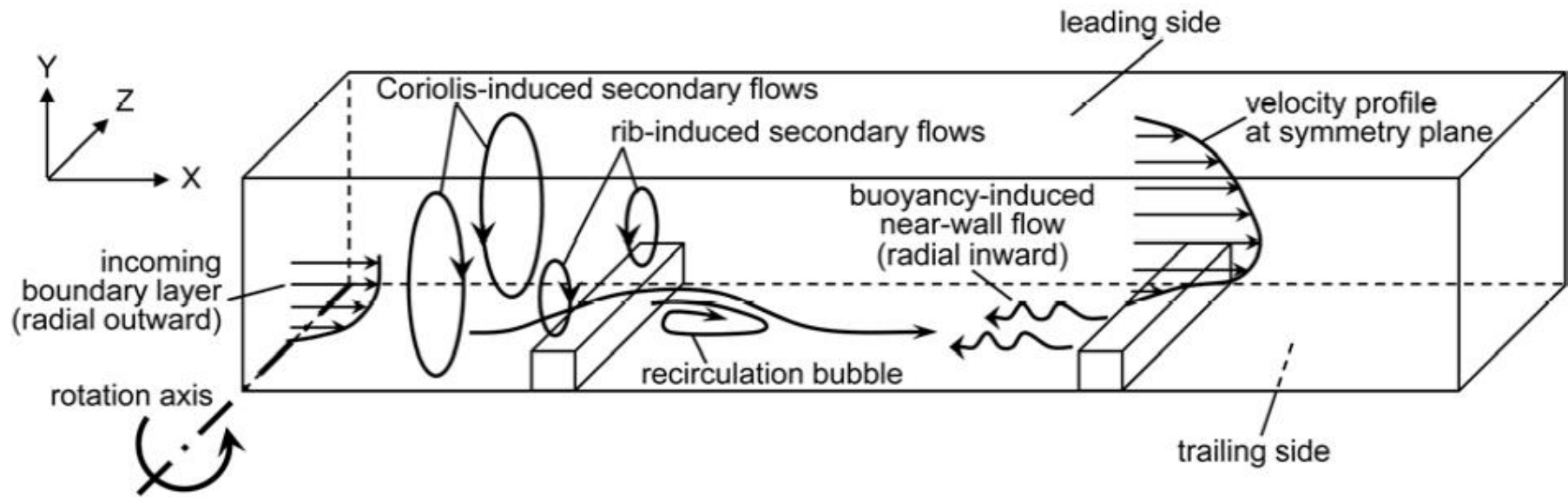
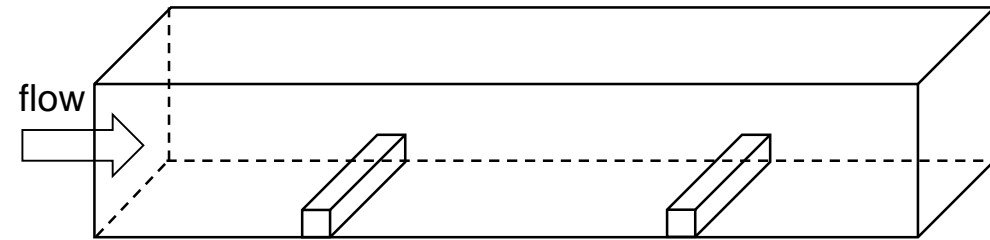
Practical contribution

- Higher TIT \rightarrow higher η_{th} & N_s
- Lower $\dot{m}_{coolant}$

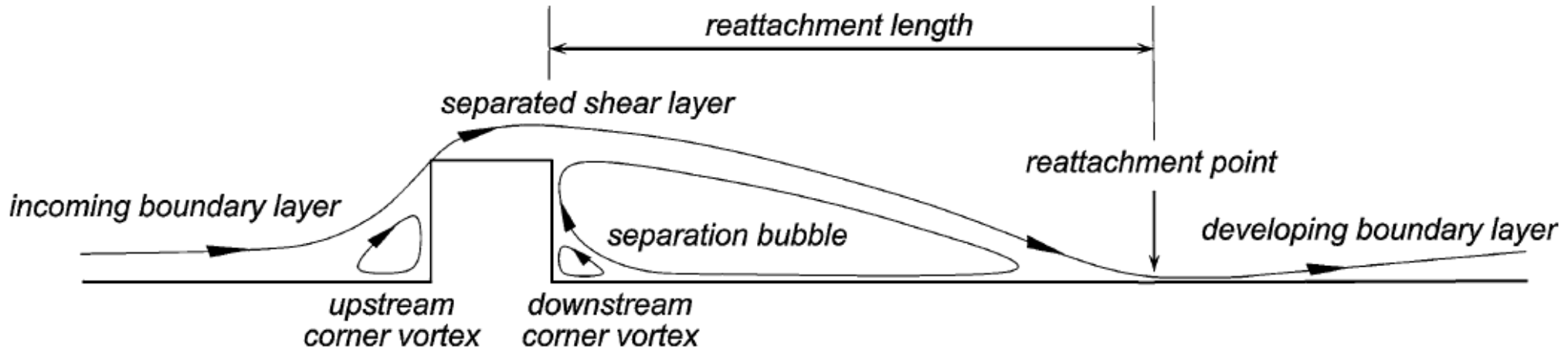
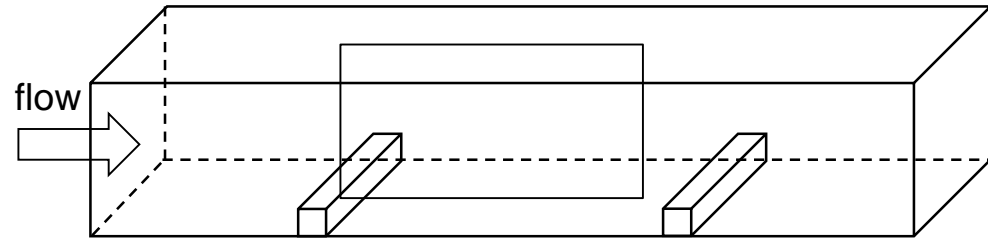


adapted from NACA rm-E54I23

Flow field



Flow field

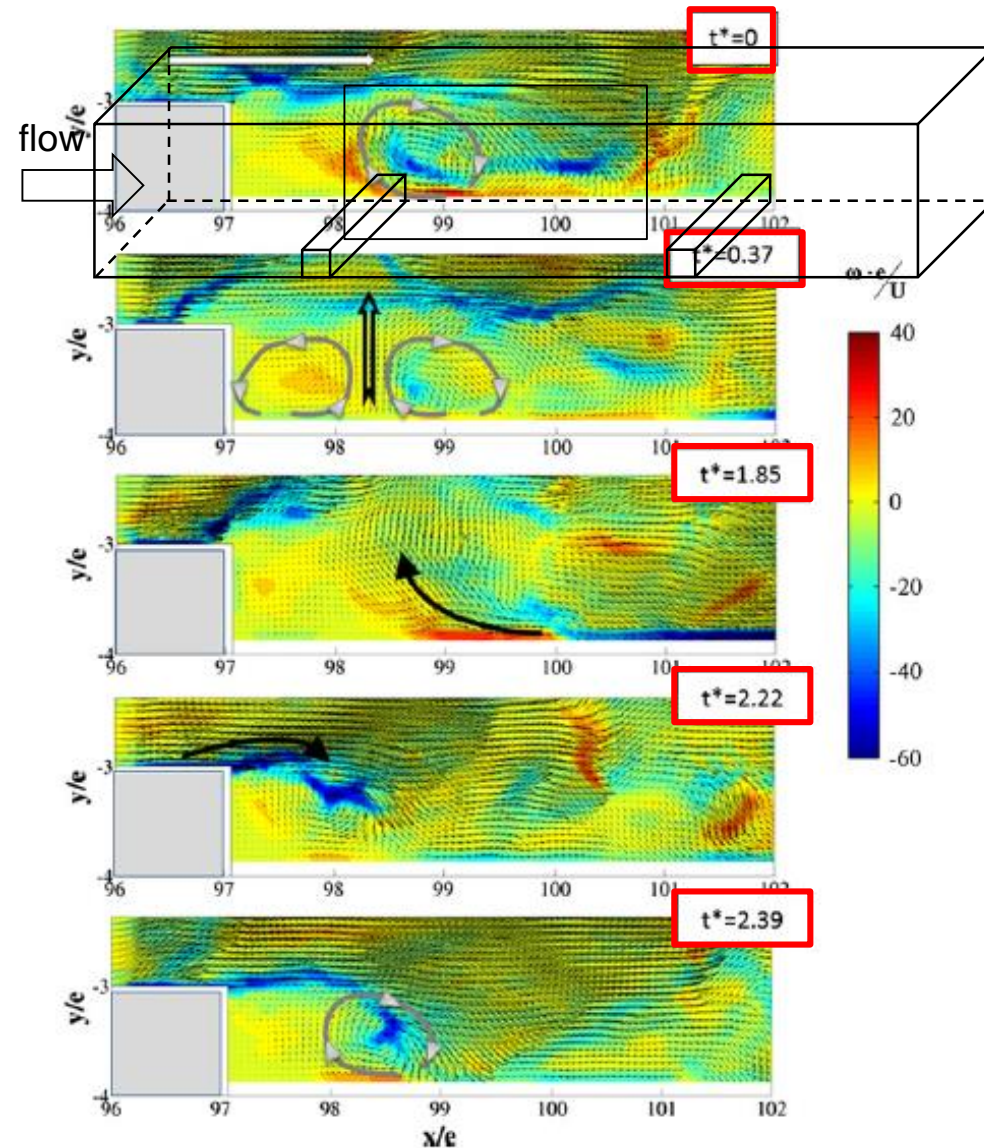


averaged internal flow field

Flow field (TR-data)

Cardwell (2011)

- rib wake at reference state
- turbulent instability of the mixing layer → 2 counter rotating vortices → relative high velocity jet
- mixing layer displacement into the core flow
- rapid ejection of the separated inter-rib region
- shear layer reorganization



Two-color LIF thermography

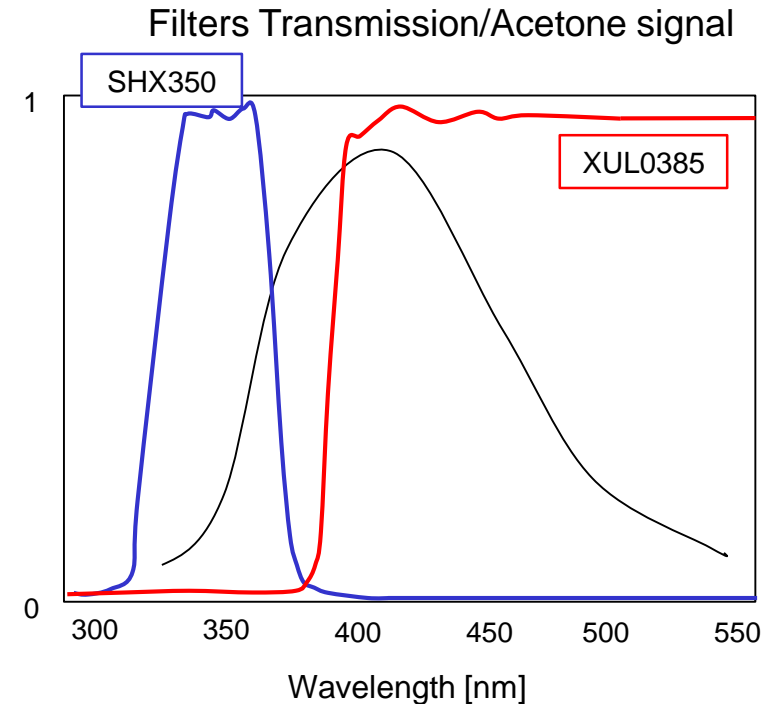
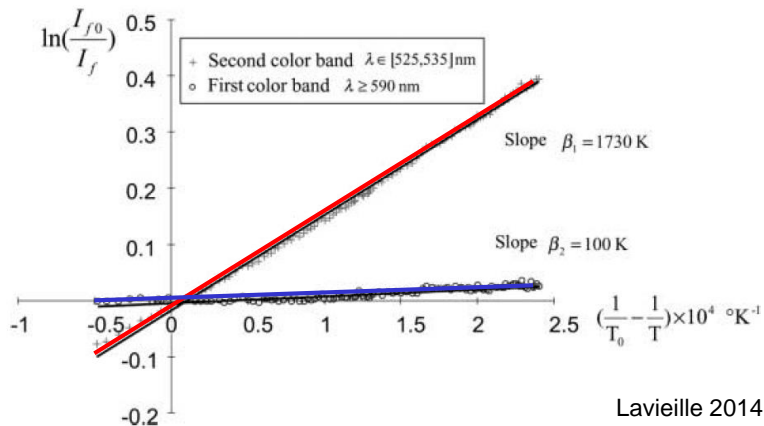
- ❑ Acetone for low toxicity, no oxygen quenching, high pressure vapour
- ❑ Filters selection with available spectral data of acetone
- ❑ Requirements
 - 1 UV laser source
 - 2 cameras

Signal

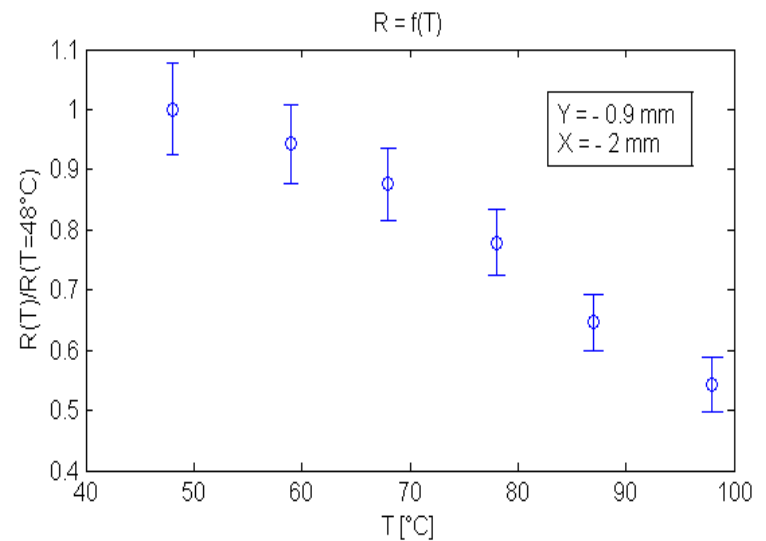
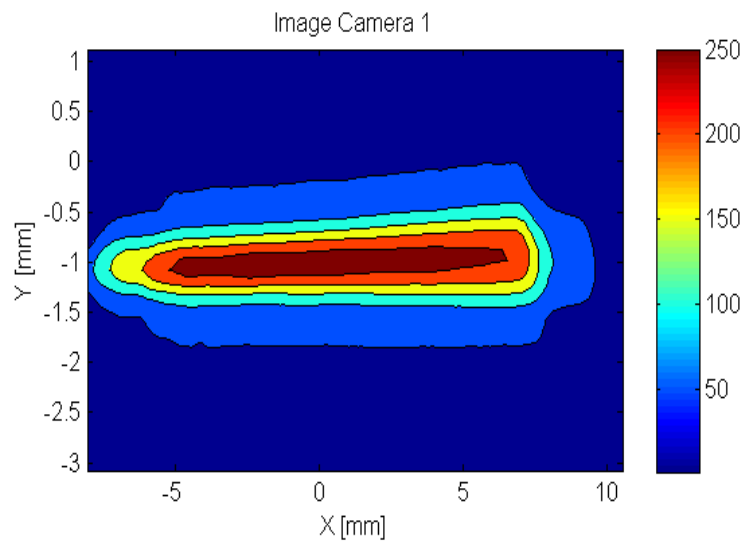
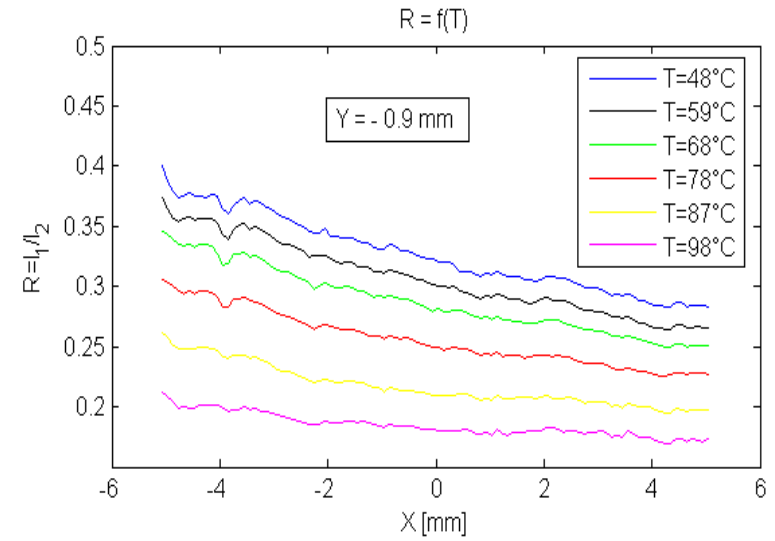
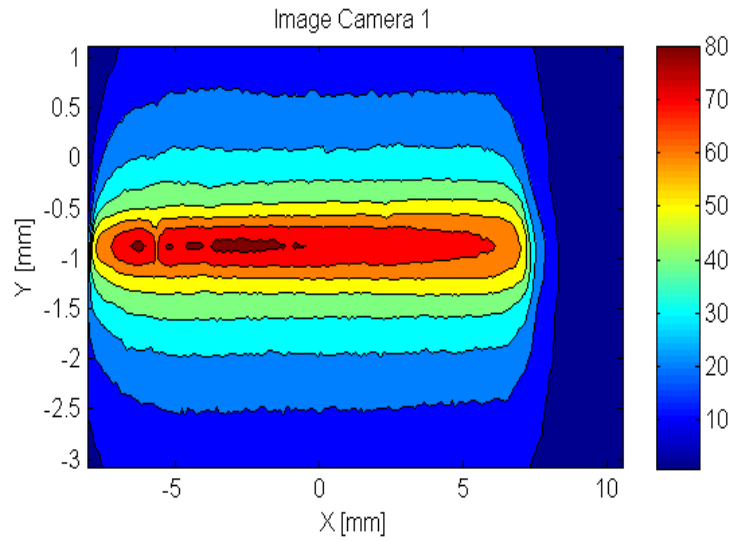
$$I_f(\lambda) = K_{opt}(\lambda)K_{spec}(\lambda)V_c I_1 C e^{\beta(\lambda)/T}$$

Intensity Ratio

$$R_f(T) = \frac{I_{f,1}}{I_{f,2}} = \frac{K_{opt,1}}{K_{opt,2}} \exp\left(\frac{\beta_1 - \beta_2}{T}\right)$$



Preliminary Study



Processing

- Background

$$I_{b,k}(i, j) = I_1(i, j) - B(i, j)$$

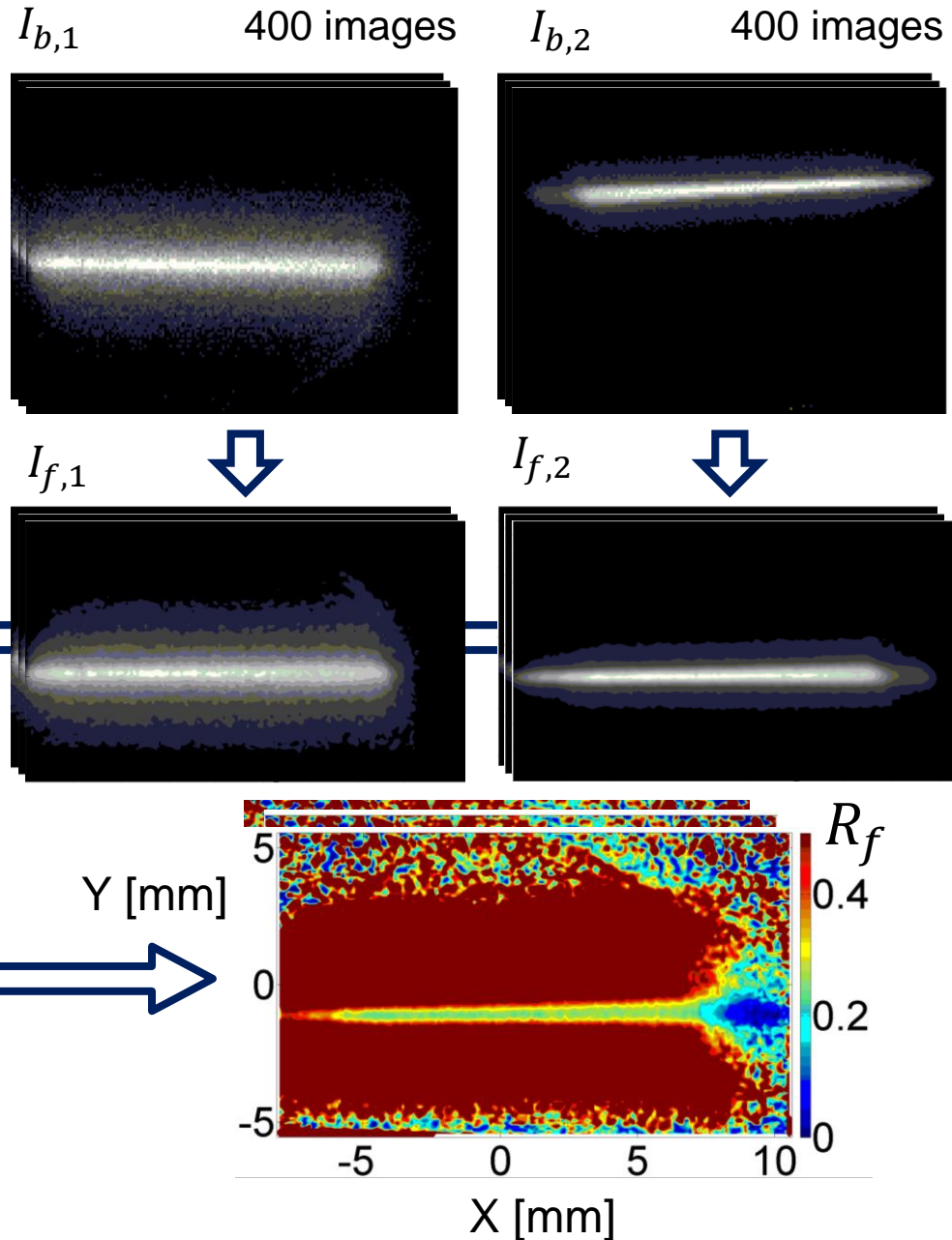
- Spatial Calibration

$$I_{f,k}(x, y) = C(i, j) \cdot I_{b,1}(i, j)$$

- Intensity ratio

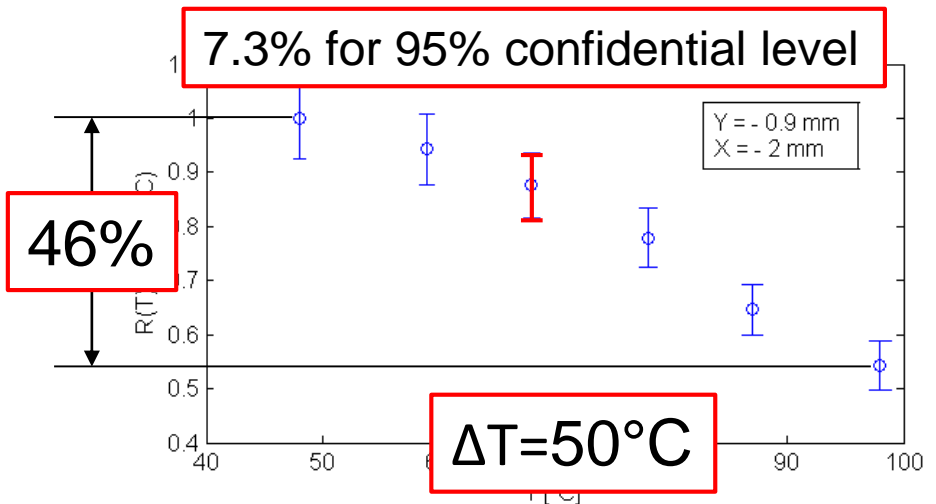
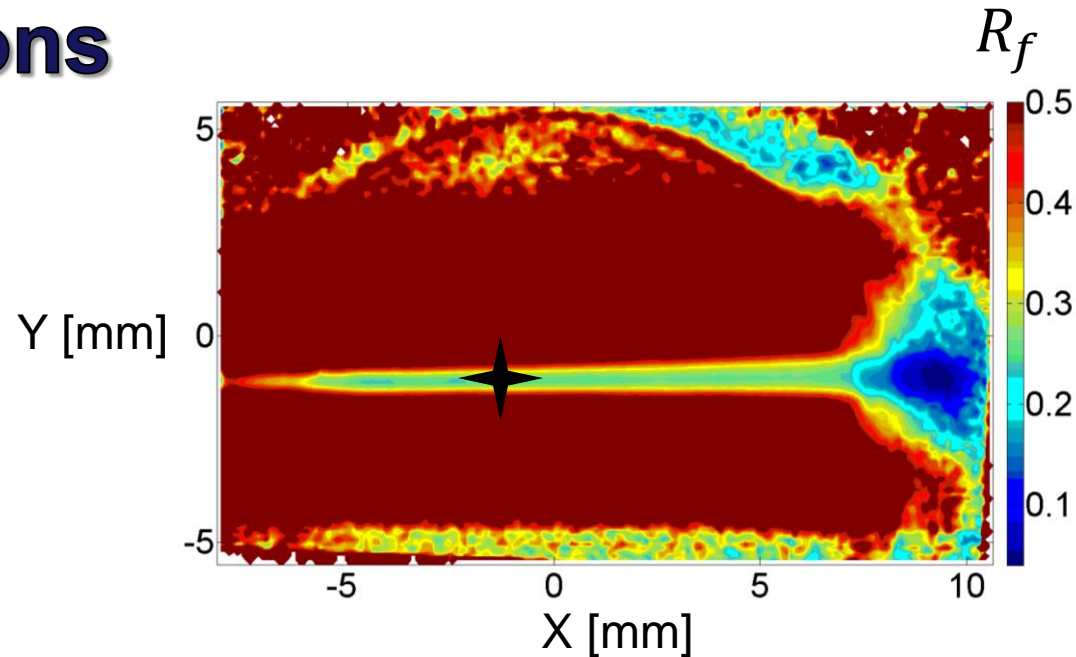
$$R_f(T) = \frac{I_{f,1}}{I_{f,2}} = \frac{K_{opt,1}}{K_{opt,2}} \exp\left(\frac{\beta_1 - \beta_2}{T} Y\right) [\text{mm}]$$

- Averaging (over 400 images per experiment)



Results and Conclusions

- ❑ 46% decrease corresponding to 50°C temperature difference
- ❑ Uncertainty of 7.3% for 95% confidence level
- ❑ Encouraging dependence of R_f with temperature but:
 - Low signal \Rightarrow high uncertainty
 - No evidence in literature (no two-color acetone studies)
- ❑ Spectral measurements of acetone fluorescence

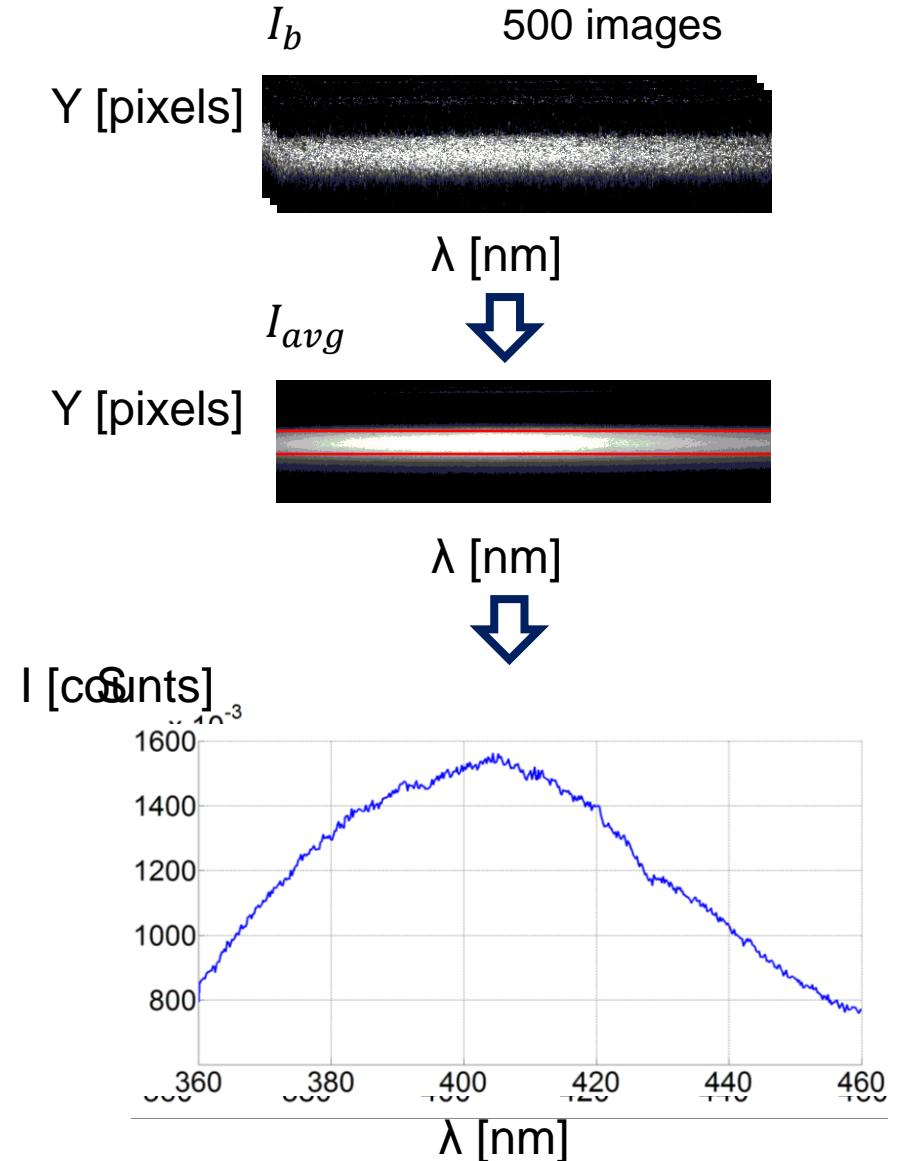


Processing

For each temperature (4) and spectral range (5)

- Background subtraction
- Laser Intensity normalization
- Average of the corrected samples
- Average in space (Y-direction) inside laser beam
- Intensity Calibration with Halogen and Tungsten lamps

$$S(\lambda) = (S_{rec}(\lambda) - BG(\lambda)) \times \frac{Cali_{rec}(\lambda) - BG(\lambda)}{Cali_{the}(\lambda)}$$



Turbulent Prandtl number

Momentum & Thermal boundary layer Equations

$$x) \quad \bar{u} \frac{\partial \bar{u}}{\partial x} + \bar{v} \frac{\partial \bar{u}}{\partial y} = -\frac{1}{\rho} \frac{d\bar{P}}{dx} + \frac{\partial}{\partial y} \left(\nu \frac{\partial \bar{u}}{\partial y} - \overline{u'v'} \right)$$

Boussinesq Approach:

$$\tau_t = \rho \mu_t \frac{\partial \bar{u}}{\partial y}$$

$$x) \quad \bar{u} \frac{\partial \bar{T}}{\partial x} + \bar{v} \frac{\partial \bar{T}}{\partial y} = \frac{\partial}{\partial y} \left(\alpha \frac{\partial \bar{T}}{\partial y} - \overline{v'T'} \right)$$

$$q_t = \rho C_p \alpha_t \frac{\partial \bar{T}}{\partial y}$$

Turbulent Prandtl Number

$$Pr_t = \frac{\mu_t}{\alpha_t}$$

by measuring $\overline{u'v'}$, $\frac{\partial \bar{u}}{\partial y}$, $\overline{v'T'}$ and $\frac{\partial \bar{T}}{\partial y}$

Validation and Modeling

Contribution for CFD

$$x) \quad \bar{u} \frac{\partial \bar{u}}{\partial x} + \bar{v} \frac{\partial \bar{u}}{\partial y} = -\frac{1}{\rho} \frac{d\bar{P}}{dx} + \frac{\partial}{\partial y} \left(\nu \frac{\partial \bar{u}}{\partial y} - \overline{u'v'} \right)$$

$$x) \quad \bar{u} \frac{\partial \bar{T}}{\partial x} + \bar{v} \frac{\partial \bar{T}}{\partial y} = \frac{\partial}{\partial y} \left(\alpha \frac{\partial \bar{T}}{\partial y} - \overline{v'T'} \right)$$

Boussinesq Approach:

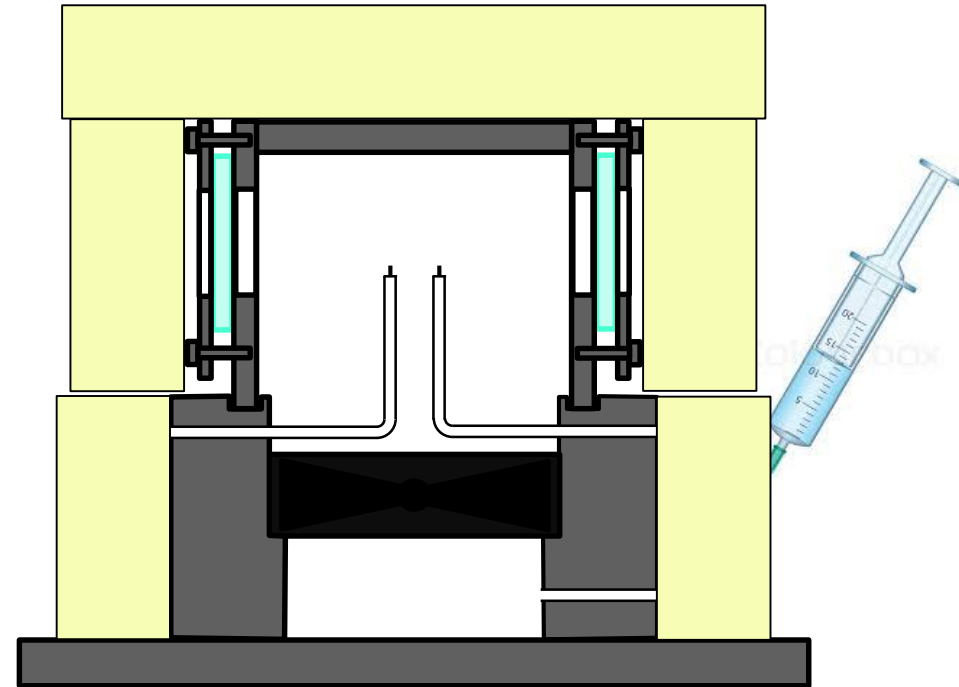
$$\overline{u'v'} = \mu_t \frac{\partial \bar{u}}{\partial y}$$

$$\overline{v'T'} = \alpha_t \frac{\partial \bar{T}}{\partial y}$$

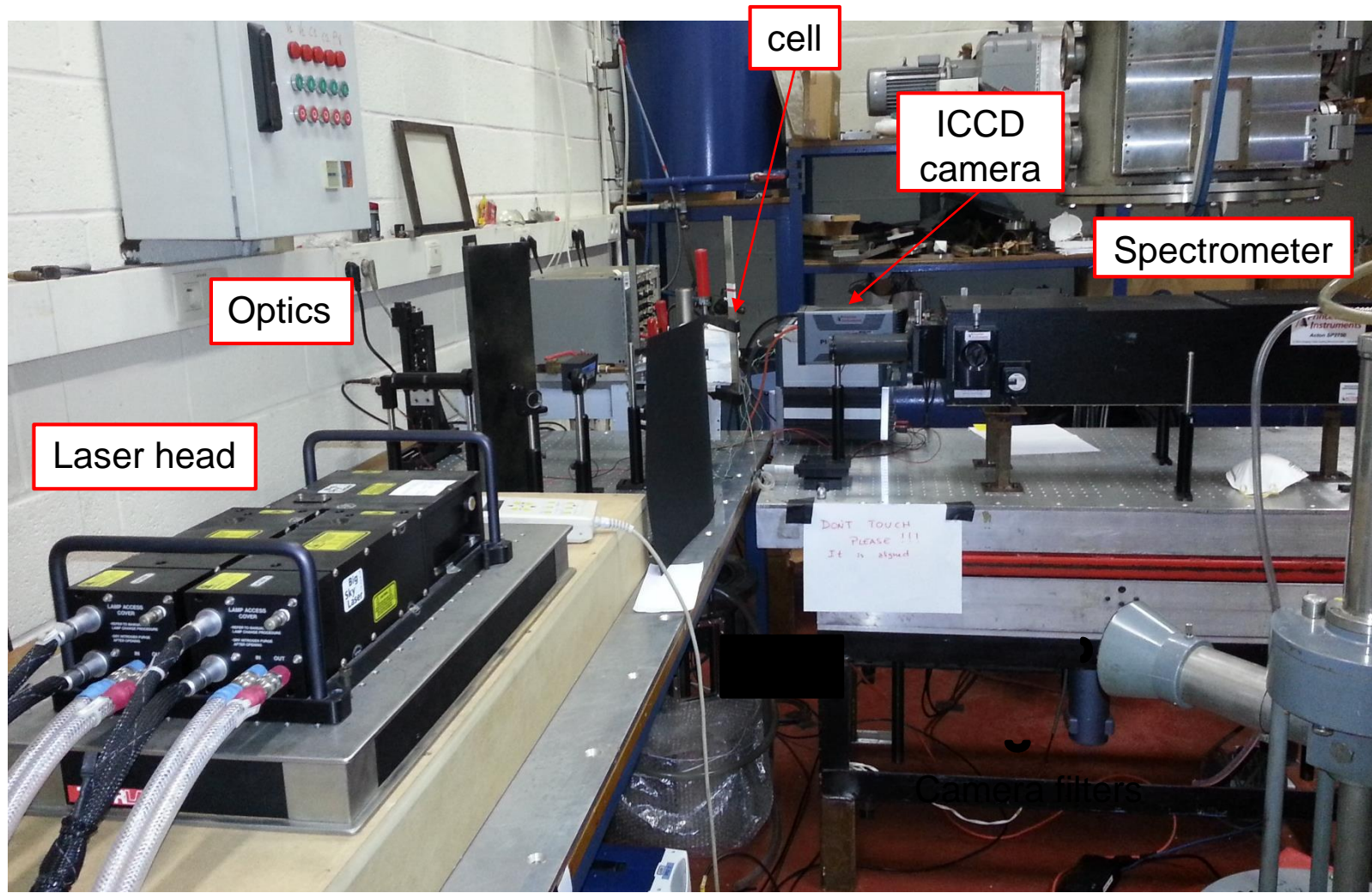
- ❑ Comparison of engineering quantities: Q (or EF), τ , ΔP_0
- ❑ Comparison of mean and rms values of velocity and thermal fields
- ❑ Direct contribution on $\overline{u'v'}$ and $\overline{v'T'}$
- ❑ $\mu_t, \alpha_t \rightarrow Pr_t = \frac{\mu_t}{\alpha_t}$

Measurement cell

- 50x50x90 mm^3 aluminum cell
- Optical accesses (laser + cameras)
- Temperature control and acquisition by 4 thermocouples
- Tracer access
- Mixing by a fan
- Thermally insulated by 15 mm layers of foam
- Heated from the bottom (heat gun)

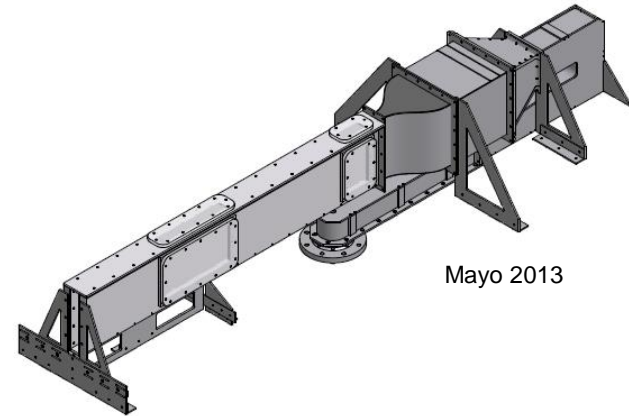


Spectral Measurement set-up



Test section for 2D internal flow

- ❑ Existing aluminum channel with high aspect ratio ($W/H = 6$)
- ❑ Embedded with Wind tunnel components
 - Diffusor
 - Settling chamber with screens and honeycomb
 - Contraction
- ❑ Re-designed optical windows with quartz slots
- ❑ Heated bottom wall by thin resistances



Mayo 2013

